AD_____

Award Number: W81XWH-05-1-0018

TITLE: Interfering with DNA damage signals: Radiosensitizing Prostate Cancer using small peptides

PRINCIPAL INVESTIGATOR: Bo Xu, MD, Ph.D.

CONTRACTING ORGANIZATION: Louisiana State University
New Orleans, LA 70112

REPORT DATE: November 2007

TYPE OF REPORT: Annual

PREPARED FOR: U.S. Army Medical Research and Materiel Command
Fort Detrick, Maryland 21702-5012

# REPORT DOCUMENTATION PAGE

*Form Approved*
*OMB No. 0704-0188*



| **1. REPORT DATE** *(DD-MM-YYYY)* | **2. REPORT TYPE** | **3. DATES COVERED** *(From - To)* |
|---|---|---|
| 01/11/07 | Annual | 1 Nov 2006 – 31 Oct 2007 |

**4. TITLE AND SUBTITLE**

Interfering with DNA damage signals: Radiosensitizing Prostate Cancer using small peptides

**5a. CONTRACT NUMBER**

**5b. GRANT NUMBER**
W81XWH-05-1-0018

**5c. PROGRAM ELEMENT NUMBER**

**6. AUTHOR(S)**
Bo Xu, MD, Ph.D.

E-Mail: xu@sri.org

**5d. PROJECT NUMBER**

**5e. TASK NUMBER**

**5f. WORK UNIT NUMBER**

**7. PERFORMING ORGANIZATION NAME(S) AND ADDRESS(ES)**

Louisiana State University
New Orleans, LA 70112

**8. PERFORMING ORGANIZATION REPORT NUMBER**

**9. SPONSORING / MONITORING AGENCY NAME(S) AND ADDRESS(ES)**
U.S. Army Medical Research and Materiel Command
Fort Detrick, Maryland 21702-5012

**10. SPONSOR/MONITOR'S ACRONYM(S)**

**11. SPONSOR/MONITOR'S REPORT NUMBER(S)**

**12. DISTRIBUTION / AVAILABILITY STATEMENT**
Approved for Public Release; Distribution Unlimited

**13. SUPPLEMENTARY NOTES**

**14. ABSTRACT:** We aimed to identify small peptides that can target critical DNA damage responsive pathways in order to develop novel therapeutic agents that can sensitize prostate cancer cells to radiotherapy. Critical DNA damage pathways determining cellular radiosensitivity is medicated by ATM and its phosphorylation of downstream targets, including Structural Maintenance of Chromosomal protein one (SMC1) and Nijmegen Breakage Syndrome protein 1 (NBS1). We have demonstrated that small fusion peptides containing SMC1 phosphorylation sequences can inhibit ATM activity. We have characterized the inhibitory effect of the THM-SMC1 peptide on cellular responses to radiation and found the peptide can abolish radiation induced S-phase checkpoint and decrease prostate tumor cell clonogenic survival. During the last performance period, we have studied the molecular mechanisms of SMC1 peptide-induced radiosensitization. We have also identified a novel inhibitory peptide containing the NBS1 C-terminal conserved sequence. The NBS1 inhibitory peptides (NIP) can increase prostate cancer cellular radiosensitivity. Future directions include in vivo evaluation of the fusion peptides as powerful radiosensitizers in prostate cancer xenograft models.

**15. SUBJECT TERMS**
ATM, SMC1, DNA damage, radiotherapy, peptide

| **16. SECURITY CLASSIFICATION OF:** | | | **17. LIMITATION OF ABSTRACT** | **18. NUMBER OF PAGES** | **19a. NAME OF RESPONSIBLE PERSON** |
|---|---|---|---|---|---|
| **a. REPORT** | **b. ABSTRACT** | **c. THIS PAGE** | | | USAMRMC |
| U | U | U | UU | 26 | **19b. TELEPHONE NUMBER** *(include area code)* |

## Table of Contents

## INTRODUCTION

Critical controllers of cellular sensitivity to ionizing radiation (IR) include the Ataxia-Telangiectasia-Mutated (ATM) protein kinase and its downstream target the Structural Maintenance of Chromosome protein one (SMC1)(Kim et al., 2002; Kitagawa et al., 2004; Yazdi et al., 2002). ATM phosphorylation of SMC1 at two serine sites is required for limiting the amount of radiation sensitivity. We have demonstrated that a small peptide containing ATM-mediated SMC1 phosphorylation sequence possesses an inhibitory effect on IR-induced SMC1 phosphorylation and S-phase checkpoint activation. Therefore we hypothesized that the peptide containing this SMC1 short sequence, when linked with an tumor homing motif (THM), can be a specific inhibitor to the ATM-mediated signaling pathway and a powerful radiosensitizer for prostate tumor radiotherapy. This hypothesis has been tested by studying the effect of synthetic peptides that aim to block the in vivo phosphorylation events on prostate cancer cellular responses to IR.

New findings have demonstrated that ATM activation is dependent upon its interaction with the NBS1 protein through NBS1 C-terminal conserved sequences (Falck et al., 2005, Cerosaletti and Concannon, 2003; Cerosaletti and Concannon, 2004; Cerosaletti et al., 2006). These new findings prompted us to explore whether targeting NBS1-ATM interactions by small peptides can achieve radiosensitization. During the last performance period, we have developed several peptides and identified an NBS1 inhibitory peptide (NIP). We have characterized the NIP peptides and concluded that disruption of NBS1-ATM interactions by wtNIP results in increased cellular radiosensitivity. Although these studies were not listed in the original Statement of Work, we considered these studies appropriate for the main hypothesis of this funded proposal, i.e. targeting critical DNA damage pathways for radiosensitization. These newly characterized peptides, along with the SMC1 fusion peptides, will be further studied for their in vivo activity of radiosensitization in prostate tumor xenograft models.

## BODY

### A. Mechanism of THM-SMC1 inhibition (Task 1).

To study if the THM-SMC1 peptide directly inhibits ATM phosphorylation of SMC1, we performed western blot analysis in DU145 prostate cancer cells treated with mock or IR (6Gy) in the absence or presence of caffeine (a non-specific ATM inhibitor) or THM peptides (THM-only, THM-wtSMC1, and THM-mtSMC1). We found that, when cells were treated with THM-wtSMC1 peptides, IR-induced SMC1 phosphorylation was significantly reduced as compared to that of cells treated with THM-only or THM-wtSMC1 (**Figure 1**). This pattern is similar to that induced by caffeine treatment, suggesting that the THM-wtSMC1 can inhibit ATM-mediated SMC1 phosphorylation.

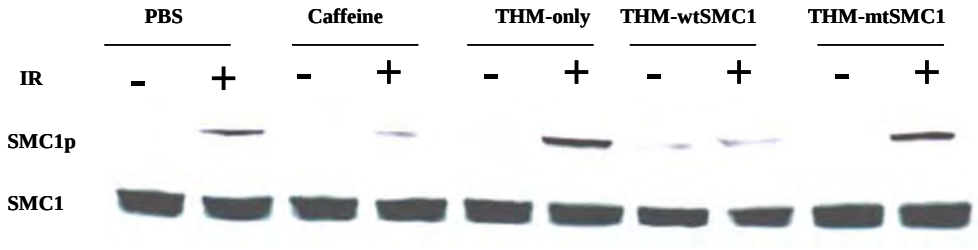


**Figure 1. The THM-wtSMC1 peptide abrogates IR-induced SMC1 phosphorylation.** DU145 were treated either with PBS, Caffeine (10mM) or the THM-fusion peptides (10uM) for 1 hour before 6Gy radiation was delivered. Two hours after radiation, total cell lysates were immunoblotted with an anti-Ser966p and an anti-SMC1 antibody..

To further test whether the THM-wtSMC1 peptide can inhibit other ATM-dependent pathways, we tested NBS1 and Brca1 phosphorylation, which are also mediated by ATM in response to IR-induced DNA damage. We found that neither NBS1 nor Brca1 phosphorylation was affected by THM-wtSMC1 peptides (**Figure 2**), demonstrating that the THM-wtSMC1 has a specific effect on ATM phosphorylation of SMC1. Since we have previously shown that the THM-SMC1 peptide can abrogate the IR-induced S-phase checkpoint, and that ATM-mediated SMC1, NBS1 and Brca1 phosphorylation is critical for activation of the checkpoint, our data indicated that SMC1 phosphorylation was a downstream event of the pathway.

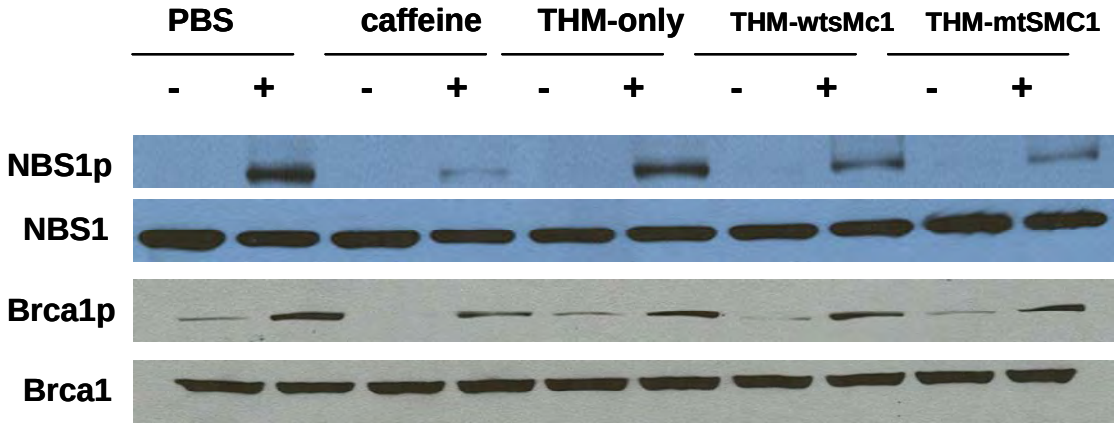


**Figure 2. THM-wtSMC1 peptide does not affect IR-induced NBS1 and Brca1 phosphorylation.** DU145 were treated either with PBS, Caffeine (10mM), or the THM-fusion peptides (10uM) for 1 hour before 6Gy radiation was delivered. Two hours after radiation, total cell lysates were immunoblotted with indicated antibodies.

**B. Identification of new inhibitory peptides (NBS1 inhibitory Peptide -NIP).**

In order to maximize the radiosensitization effect of small inhibitory peptides, we have continued to identify novel peptides that can target the DNA damage responsive pathways Recent studies have revealed that the C-terminal NBS1 domain is critical for binding to ATM (Falck et al., 2005). An NBS1 truncated derivative lacking the C-terminal 20 residues does not associate with ATM *in vitro* (Cerosaletti and Concannon, 2003; Cerosaletti and Concannon, 2004; Cerosaletti et al., 2006). In addition, it has recently been shown that expression of an NBS1 transgene lacking the ATM binding domain in NBS cells leads to a dramatic reduction in ATM activation (Difilippantonio et al., 2005). Therefore NBS1-ATM interaction can be an appealing target for developing radiosensitizers, since inhibiting NBS1 association with ATM leads to suboptimal ATM activation after IR, thereby sensitizing cells to radiation. One approach to inhibiting NBS1-ATM interaction would be to use small peptides containing the conserved C-terminal sequence of NBS1 which can presumably compete with endogenous NBS1-ATM interaction. To test this hypothesis, we generated several fusion peptides using a polyarginine sequence ($R_9$) for internalization. These include the polyarginine ($R_9$) internalization sequence alone, and a wild-type NBS1 inhibitory peptide (wtNIP) corresponding to amino acids 734-748 of human

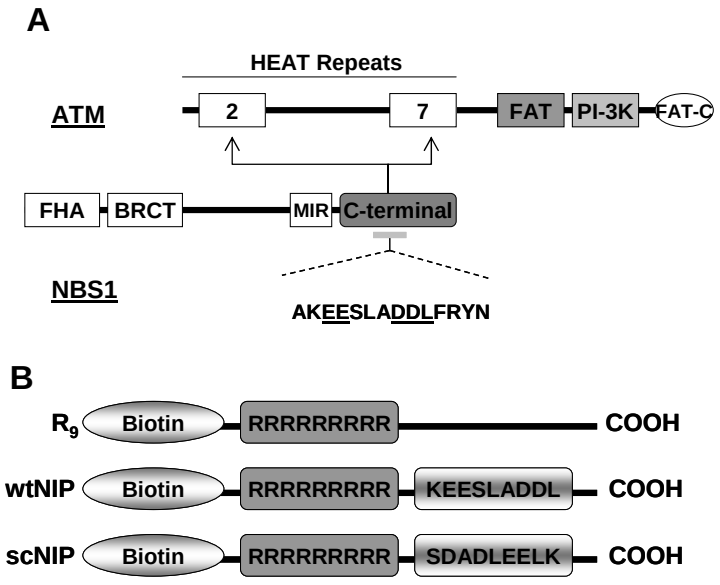


**Figure 3. Development of the NBS1 Inhibitory Peptides (NIPs).** *A.* Schematic illustration of functional domains of ATM an NBS1 and their interaction. The C-terminal of NBS1 is required for ATM activation and recruitment to sites of DNA damage. It consists of at least two sets of amino acid residues, 736-737 (EE) and 741-742 (DDL), that are evolutionarily conserved and necessary for ATM binding. NBS1 binds to two sets of Heat Repeats (Heat Repeat 2 (a.a. 248-522), and Heat Repeat 7 (a.a.1436-1770), in ATM. *B.* The amino acid sequences for the R9, wtNIP, and scNIP peptides developed.

NBS1. To serve as a negative control, we used a random sequence generator to produce a peptide in which a.a. 734-748 of human NBS1 were scrambled (scNIP) as shown in **Figure 3**. $R_9$, wtNIP and scNIP were synthesized and labeled with a biotin tag at their N-terminus for detection *in vitro*. Cells treated with the peptide were probed with a fluorescein-conjugated streptavidin antibody to determine the presence of the biotinylated peptides. Our data demonstrated that cells treated with $R_9$, wtNIP, and scNIP display significant cytoplasmic and nuclear localization (data not shown, see appendix).

We then set out to determine the length of time the peptides remain in cells as a way to ensure the peptides would be present throughout the DNA repair process after IR. As shown in **Figure 4**, immediately after incubation with the peptides, all sample groups show distinct presence of peptides. Within 2 hours of treatment cells continue to display a strong distribution of $R_9$, wtNIP and scNIP but fluorescent intensity levels of wtNIP and scNIP begin to decrease within 4 hours with a substantial decline by 8 hrs. $R_9$ fluorescence remains slightly elevated at 8 hours while wtNIP and scNIP intensities are much weaker. This is in agreement with literature which suggests that $R_9$ sequences translocate easier and remain present longer than when they are not coupled to a molecule or peptide (Jones et al., 2005). By 12 hours, cells treated with $R_9$ peptides still display prominent staining, while cells treated with wtNIP or scNIP show much weaker cytoplasmic staining with no observed nuclear staining. Within 24 hours, cells treated with $R_9$ show cytoplasmic staining, but the nuclear signal is no longer visible, cells treated with wtNIP or scNIP show no detectable presence of the peptides. These data suggest that the NIP peptides should be added to cells every 4-6 hours in the first 24 hours after treatment with IR in order to achieve maximal inhibitory effects.

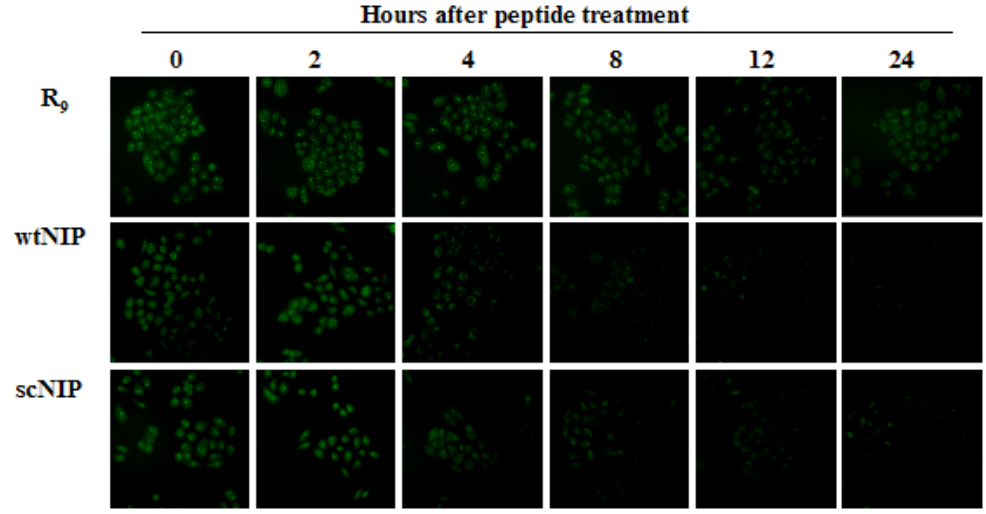


**Figure 4. Degradation of the R9, wtNIP or scNIP peptides**. HeLa cells were treated with 10μM R9, wtNIP, or scNIP for one hour and harvested at indicated time points before they were analyzed by immunofluorescence microscopy staining with an anti-streptavidin antibody.

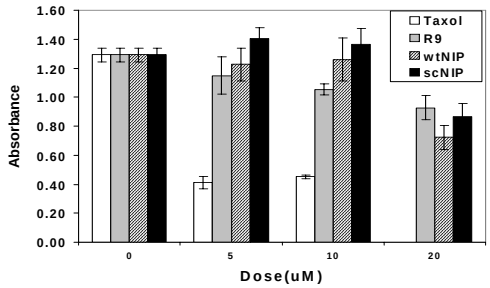


**Figure 5. The cytotoxicity of the NIP peptides.** Hela cells were treated Taxol and the NIP peptides at indicated doses. 24 hours after treatment, cell survival was quantified by a standard MTT assay.

### C. Peptide Cytotoxicity

An ideal candidate for a radiosensitizer should possess little or no cytotoxicity by itself in order for investigations to purely assess the radiosensitizing effect on tumor cells. To test the cytotoxicity of the peptides, HeLa cells were treated with $R_9$, wtNIP or scNIP for 24h at

ambient temperature. After incubation, media containing peptides was removed, fresh media added and the cultures incubated for additional 24 hours. At the end of the time course, the commercially available MTT cell viability assay (Promega Corp., Madison WI) was used to determine peptide cytotoxicity. A chemotherapeutic agent Taxol (from Sigma) was used as a positive control. Our data show that the NIP peptides possess minimal cytotoxicity to cells in doses below 10μM (**Figure 5**). Clonogenic surviving assays confirmed a minimal toxicity of the peptides (data not shown). A dose-response and time course experiments were also performed and repeated in other cell lines (data not shown), and the conclusion is firmed.

**D. wtNIP inhibits IR-induced γ-H2AX and NBS1 focus formation.**

One of the earliest responses after DNA damage is the formation of γ-H2AX foci at sites of DSBs, an event that requires functional ATM (Burma et al., 2001; Furuta et al., 2003). Since the wtNIP peptide was designed to interfere with NBS1-ATM interaction and ATM activation, we investigated whether IR-induced γ-H2AX focus formation was inhibited by the peptide. Immunofluorescence microscopy was used to detect the presence of γ-H2AX foci in mock or irradiated cells in the presence of 10μM $R_9$, wtNIP or scNIP. We observed that while $R_9$ showed no inhibition on γ-H2AX focus formation, wtNIP significantly diminished IR-induced γ-H2AX foci (Figure 6). The scNIP peptide did not have any effects on IR-induced focus formation, suggesting that only wtNIP can display an inhibitory effect in the DNA damage response. These observations have been confirmed in other cell lines, including the prostate cancer cell line DU-145 (data not shown, see appendix)

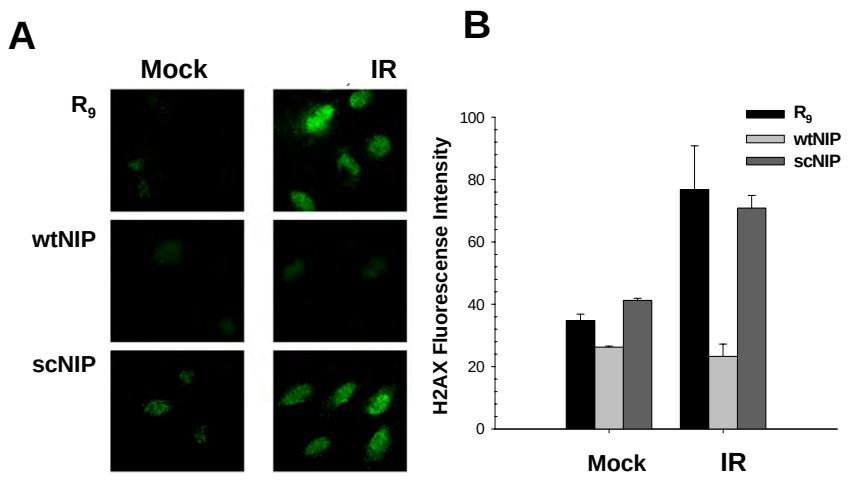


**Figure 6. wtNIP can inhibit γ-H2AX foci formation. A.** Hela cells were treated with 10μM R9, wtNIP, or scNIP for 1hour, irradiated with 0 or 6Gy, and harvested 30 minutes later before immunofluorescence microscopy was employed to detect radiation induced-γ-H2AX foci. **B.** The mean γ-H2AX fluorescence intensity was determined for each image using Image Pro 5.1 software and is expressed in arbitrary units. Error bars represent +/- 1 SD, graphed are the mean of three independent experiments

To further support our conclusion, we investigated IR-induced NBS1 focus formation, an event considered to be an ATM-dependent process at the sites of DSBs (Lim et al., 2000). NBS1 foci are a result of ATM-mediated NBS1 phosphorylation on Serine 343. Using an anti-phospho-Ser343 NBS1 antibody, we observed that NBS1 phosphorylation was significantly inhibited in cells treated with wtNIP compared to those treated with $R_9$ or scNIP (data not shown, see appendix). The average number of foci in mock-irradiated cells was 5.96, 7.96, and 5.88 for 10μM $R_9$, wtNIP, and scNIP respectively. Cells treated with $R_9$ or scNIP displayed average foci of 24.52 and 30.84, while cells treated with wtNIP showed only 6 foci per nucleus 2hrs after treatment with 6Gy IR (data not shown, see appendix). These observations demonstrate that the wtNIP peptide can inhibit the ATM-mediated signaling pathway.

**E. wtNIP increases radiation sensitivity.**

The clonogenic survival assay was then used as a tool for determining *in vitro* radiosensitivity of cultured mammalian cells. To characterize the radiosensitizing potential of our peptides, Hela or DU-145 cells were plated in six-well plates at limiting dilutions, treated with either DMEM or 10μM $R_9$, wtNIP, or scNIP and mock irradiated or irradiated with 2-6Gy. At 6-8 hr intervals for 24 hrs following irradiation, fresh peptides were added, and colonies allowed to grow for 10-12 days. When Hela or DU-145 cells were treated with 10μM wtNIP, both cell lines demonstrated a marked increase in radiosensitization with a significant difference observed in wtNIP and DMEM, $R_9$, or scNIP treated cells (Shown in Figure 7A is the surviving curve of Hela cells, DU-145 data not shown). Radiation survival curves were then characterized based on $D_0$ to define the NIP's effect on radiosensitivity. $D_0$ represents the mean lethal dose which kills 63% of the cells and is a measure of the intrinsic radiosensitivity of the cell. The smaller the $D_0$ value, more radiosensitive the cell line. $D_0$ values for Hela and DU-145 treated with wtNIP were 1.9 and 2.4 compared to 3.0 and 3.4 for cells treated with scNIP. To better determine the radiosensitizing potential of the peptides in comparison to other small molecule inhibitors, we calculated the sensitizing enhancement ratio (SER) based on the following formula:

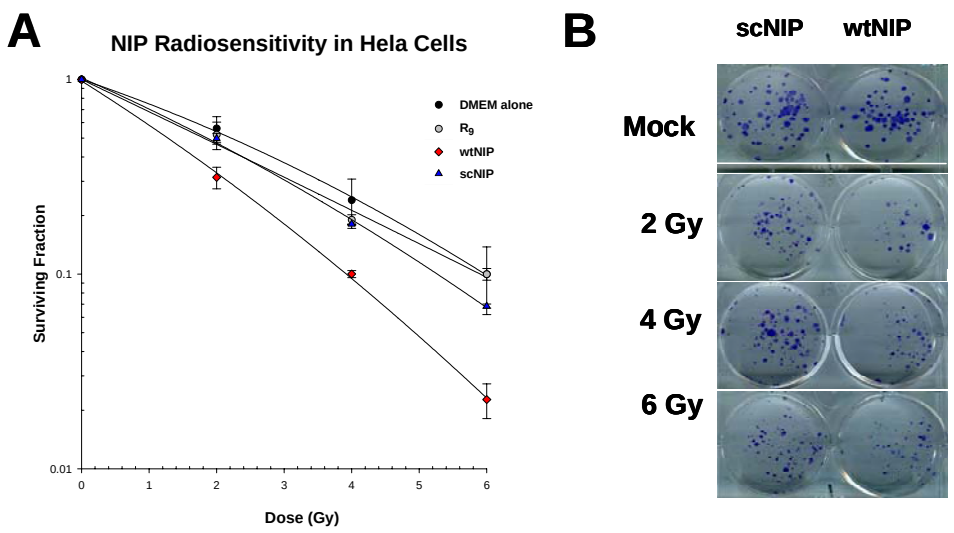


**Figure 7. wtNIP increases cellular radiosensitivity.** HeLa cells were seeded at limiting dilutions and treated with 10μM R9, wtNIP, or scNIP for one hour prior to irradiation, harvested 10-12 days later and stained with crystal violet. Shown in A is the surviving curve after indicated doses of radiation. Error bars represent +/- 1 SD, graphed are the mean of three independent experiments. ***B.*** Representative plates of the clonogenic assay for NIP mediated radiosensitivity.

$$SER = \frac{\text{Surviving fraction at 2Gy of untreated group}}{\text{Surviving fraction at 2Gy of treated group}}$$

The SER for HeLa cells was 1.8 and for DU-145 was 1.5. These values are comparable to other tested radiosensitizers, including Gemcitabine, 5-Fluorouracil, Pentoxifylline, and Vinorelbine with SERs from 1.1-2.5 (Lawrence et al., 2001; Robinson et al., 2003; Strunz et al., 2002; Araki et al., 2003). These are also comparable to ATM-specific radiosensitizers listed in Table 1.

To establish the statistical significance of wtNIP-induced radiosensitivity, Student's t-test (Paired 2 sample for means) was incorporated. The data were first fit to each experimental group over a dose range of 0-6Gy. Significant differences ($p<0.05$) in clonogenic survival were observed between cells treated with wtNIP, and those treated with DMEM, $R_9$, or scNIP. Collectively, these observations provide strong evidence for the radiosensitizing potential of the wtNIP peptide.

## KEY RESEARCH ACCOMPLISHMENTS

1. We have demonstrated that the THM-wtSMC1 peptide can specifically target the ATM-SMC1 pathway in response to DNA damage.
2. We have identified a novel inhibitory peptide (wtNIP) that specifically interfered with the NBS1-ATM interaction in the DNA damage responses.
3. The wtNIP peptide can abrogate IR-induced H2AX and NBS1 focus formation and increase radiosensitivity in prostate cancer cells.

## REPORTABLE OUTCOMES

### A. Publications and meeting presentations:

1. Mickael Cariveau, Jessie Tang, Xiaoli Cui, and Bo Xu. Conserved NBS1 C-terminal small peptides can inhibit the ATM-mediated DNA damage response and enhance radiation sensitivity. *Molecular Pharmacology*, AUG 2007, 72 (2): 320-326.
2. Xi Tang, Zhou-guang Hui, Xiao-li Cui, Renu Garg, Michael B. Kastan, and Bo Xu. A novel ATM-dependent pathway regulates Protein Phosphatase 1 and histone H3 phosphorylation in response to DNA damage. *Molecular Cellular Biology*. April 4, 2008, 2559-2566
3. Mickael J. Cariveau, Xiao-Li Cui and Bo Xu， Interfering with NBS1-ATM Interaction to Inhibit the DNA Damage Response and Sensitize Tumor Cells to Radiation. Presented in the 98th Annual meeting of American Association for Cancer Research, Los Angeles, CA, April 2007

### B. Awards/honors:

The John R. Durant Award for Excellence in Cancer Research (Junior Faculty Category, 3rd place), University of Alabama at Birmingham Comprehensive Cancer Center Annual Scientific Retreat Competition, October, 2006

### C. Invited seminars/lectures:

1. “Recent Advances in Cancer Drug Discovery”, Samford University School of Pharmacy, March 12, 2008
2. “Modern Molecular Radiobiology: Molecular targeted Radiosensitization”, Department of Radiation Oncology, The Methodist Hospital, Houston, TX. March 19, 2008
3. “DNA damage response mechanisms, from fundamental biology to cancer drug discovery”, The Methodist Hospital Research Institute, Houston, TX. March 20, 2008
4. “Roles of ATM in DNA damage response”, The 2nd International Conference on Frontiers in Biomedical and Environmental Health Sciences: DNA Repair and Cancer Biology. April 16-20, 2008, Hangzhou, China
5. “Targeting DNA damage pathways by small inhibitory peptides”, 1st Annual World Congress of ibio2008, Hangzhou, China, May 19, 2008 (also served as session co-chair)
6. “Roles of ATM phosphorylation of Inhibitor 2 in response to DNA damage”, FASEB Summer Research Conference (10th biannual phosphatase meeting), Snowmass Village, CO, July 15, 2008

## CONCLUSIONS

We have identified two types of small peptides that can interfere with DNA damage-induced signaling pathways mediated by ATM. The THM-wtSMC1 can abrogate ATM-dependent SMC1 phosphorylation, and the wtNIP peptide can abrogate NBS1-ATM interactions and IR-induced H2AX and NBS1 focus formation. These peptides can increase prostate cancer radiosensitivity. Future experiments will focus on testing whether these peptides are synergistic in combination with radiation and whether they have in vivo radiosensitization activity.

## REFERENCES


Araki,J., Nishio,K., Watanabe,M., and Oda,T. (2003). [Combination therapy with vinorelbine and gemcitabine in unresectable non-small cell lung cancer]. Gan To Kagaku Ryoho *30*, 837-839.

Burma,S., Chen,B.P., Murphy,M., Kurimasa,A., and Chen,D.J. (2001). ATM phosphorylates histone H2AX in response to DNA double-strand breaks. J. Biol. Chem. *276*, 42462-42467.

Cerosaletti,K. and Concannon,P. (2004). Independent roles for nibrin and Mre11-Rad50 in the activation and function of Atm. J. Biol. Chem. *279*, 38813-38819.

Cerosaletti,K., Wright,J., and Concannon,P. (2006). Active role for nibrin in the kinetics of atm activation. Mol. Cell Biol. *26*, 1691-1699.

Cerosaletti,K.M. and Concannon,P. (2003). Nibrin forkhead-associated domain and breast cancer C-terminal domain are both required for nuclear focus formation and phosphorylation. J. Biol. Chem. *278*, 21944-21951.

Difilippantonio,S., Celeste,A., Fernandez-Capetillo,O., Chen,H.T., Reina,S.M., Van Laethem,F., Yang,Y.P., Petukhova,G.V., Eckhaus,M., Feigenbaum,L., Manova,K., Kruhlak,M., Camerini-Otero,R.D., Sharan,S., Nussenzweig,M., and Nussenzweig,A. (2005). Role of Nbs1 in the activation of the Atm kinase revealed in humanized mouse models. Nat. Cell Biol. *7*, 675-685.

Falck,J., Coates,J., and Jackson,S.P. (2005). Conserved modes of recruitment of ATM, ATR and DNA-PKcs to sites of DNA damage. Nature *434*, 605-611.

Kim,S.T., Xu,B., and Kastan,M.B. (2002). Involvement of the cohesin protein, Smc1, in Atm-dependent and independent responses to DNA damage. Genes Dev. *16*, 560-570.

Kitagawa,R., Bakkenist,C.J., McKinnon,P.J., and Kastan,M.B. (2004). Phosphorylation of SMC1 is a critical downstream event in the ATM-NBS1-BRCA1 pathway. Genes Dev. *18*, 1423-1438.

Lim,D.-S., Kim,S.-T., Xu,B., Maser,R.S., Lin,J., Petrini,J.H.J., and Kastan,M.B. (2000). ATM phosphorylates p95/nbs1 in an S-phase checkpoint pathway. Nature *404*, 613-617.

Lawrence,T.S., Davis,M.A., Hough,A., and Rehemtulla,A. (2001). The role of apoptosis in 2',2'-difluoro-2'-deoxycytidine (gemcitabine)-mediated radiosensitization. Clin. Cancer Res. *7*, 314-319.

Robinson,B.W., Im,M.M., Ljungman,M., Praz,F., and Shewach,D.S. (2003). Enhanced radiosensitization with gemcitabine in mismatch repair-deficient HCT116 cells. Cancer Res. *63*, 6935-6941.

Yazdi,P.T., Wang,Y., Zhao,S., Patel,N., Lee,E.Y., and Qin,J. (2002). SMC1 is a downstream effector in the ATM/NBS1 branch of the human S-phase checkpoint. Genes Dev. *16*, 571-582.

## Appendices

Publications:

1. Mickael Cariveau, Jessie Tang, Xiaoli Cui, and Bo Xu. Conserved NBS1 C-terminal small peptides can inhibit the ATM-mediated DNA damage response and enhance radiation sensitivity. Molecular Pharmacology, AUG 2007, 72 (2): 320-326.
2. Xi Tang, Zhou-guang Hui, Xiao-li Cui, Renu Garg, Michael B. Kastan, and Bo Xu. A novel ATM-dependent pathway regulates Protein Phosphatase 1 and histone H3 phosphorylation in response to DNA damage. Molecular Cellular Biology. April 4, 2008, 2559-2566

0026-895X/07/7202-320–326$20.00
MOLECULAR PHARMACOLOGY
Vol. 72, No. 2
36681/3234364
*Mol Pharmacol* 72:320–326, 2007
*Printed in U.S.A.*




# Characterization of an NBS1 C-Terminal Peptide That Can Inhibit Ataxia Telangiectasia Mutated (ATM)-Mediated DNA Damage Responses and Enhance Radiosensitivity[S]

Mickael J. Cariveau, Xi Tang, Xiao-Li Cui, and Bo Xu

*Department of Biochemistry and Molecular Biology, Southern Research Institute (M.J.C., X.-L.C., B.X.) and Comprehensive Cancer Center (M.J.C., X.-L.C., B.X.), University of Alabama at Birmingham, Birmingham, Alabama; and Department of Genetics, Louisiana State University Sciences Center, New Orleans, Louisiana (X.T.)*

Received April 3, 2007; accepted May 16, 2007

## ABSTRACT

ATM and NBS1, mutation of which lead to the human autosomal recessive diseases ataxia telangiectasia and Nijmegen breakage syndrome (NBS), respectively, are essential elements in the cellular response to DNA damage induced by ionizing radiation (IR). ATM is a member of the phosphatidylinositol 3-kinase family and is activated by IR in an NBS1-dependent manner. The extreme C terminus of NBS1 contains an evolutionarily conserved sequence motif that is critical for binding to and activation of ATM after IR. ATM phosphorylates a series of targets to initiate cell cycle arrest and promote cell survival in response to DNA damage. Therefore, targeting the NBS1-ATM interaction may lead to a novel approach for specific ATM inhibition and radiosensitization. We developed small peptides containing the conserved C-terminal sequence of NBS1 to investigate whether these peptides can interfere with the DNA damage pathway. We found that wild-type NBS1 inhibitory peptides (wtNIP) can abrogate NBS1-ATM association in the presence or absence of IR. We also found that cells exposed to wtNIP displayed a significant reduction in radiation-induced $\gamma$-H2AX and NBS1 focus formation compared with cells treated with control peptides, demonstrating that wtNIP possesses a strong inhibitory effect on ATM. The inhibitory effect of wtNIP also leads to a significant decrease in clonogenic survival in response to IR. Furthermore, wtNIP does not radiosensitize cells with defective ATM, suggesting a specific inhibition of ATM. Together , these data provide a proof of principle for the use of NBS1 C-terminal small peptides as specific ATM inhibitors and radiosensitizers.

The DNA damage response is controlled by a concise series of signaling events that result in activation of cell cycle checkpoints, DNA repair, and apoptosis. This network is composed of a number of gene products, which include sensors, transducers, and effectors. DNA double-strand breaks (DSBs) are detected by sensor molecules that trigger the activation of transducing kinases. Transducers then amplify the signals by phosphorylation of effector molecules to regulate the signaling cascades that initiate cell cycle checkpoints, influence DNA repair machinery, or trigger apoptotic pathways. One central element in the network is the *ATM* gene, mutation of which contributes to the human autosomal recessive disorder ataxia-telangiectasia (A-T) (Shiloh, 2003). A-T is characterized by progressive neurodegeneration, variable immunodeficiency, an extremely high predisposition to the development of lymphoid malignancies, and a hypersensitivity to IR. Cells derived from patients with A-T show a variety of abnormalities, including cell cycle checkpoint defects, chromosomal instability, and hypersensitivity in response to IR. *ATM* is remarkable for its large size and the existence of a sequence in its carboxyl terminus similar to phosphatidylinositol 3-kinases. A family of genes, including *Tel1*, *Mec1*, and *Rad3* in yeast, *Mei-41* in *Drosophila melanogaster*, and *ATR* and *DNA-PK* in vertebrates, are similar in size and presence of the carboxyl terminal kinase sequence

This work was supported in part by grants from the National Institutes of Health (RR020152-01 and ES013301), the Department of Defense (W81XWH-05-1-0018), and the Strategic Investment Plan of Southern Research Institute.
Article, publication date, and citation information can be found at http://molpharm.aspetjournals.org.
doi:10.1124/mol.107.036681.
[S] The online version of this article (available at http://molpharm.aspetjournals.org) contains supplemental material.

**ABBREVIATIONS:** DSB, double-strand break; A-T, ataxia-telangiectasia; IR, ionizing radiation; HEAT, huntingtin/elongation factor 3/the 65 kDa $\alpha$-regulatory subunit of protein phosphatase 2A/yeast PI-3K TOR1; MRN, Mre11-Rad50-NBS1 complex; NBS1, Nijmegan breakage syndrome; ATM, ataxia telangiectasia mutated; DMEM, Dulbecco's modified Eagle's media; FBS, fetal bovine serum; NIP, NBS1 inhibitory peptide; wtNIP, wild-type NBS1 inhibitory peptide; scNIP, scrambled NBS1 inhibitory peptide; MTT, 3-(4,5-dimethylthiazol-2-yl)-2,5-diphenyltetrazolium; SER, sensitizing enhancement ratio; ATR, ataxia telangiectasia related; DNA-PKcs, DNA-dependent protein kinase catalytic subunit; siRNA, small interfering RNA; LY294002, 2-(4-morpholinyl)-8-phenyl-4*H*-1-benzopyran-4-one; KU55933, 2-morpholin-4-yl-6 thianthren-1-yl-pyran-4-one.

and are all involved in controlling DNA damage response (Abraham, 2001). The functional domains of the ATM protein include several HEAT repeats that act as scaffolding for assembly of molecular components, a phosphatidylinositol 3-like kinase domain that can phosphorylate serine/threonine followed by glutamine (the S/T-Q consensus sequence), and a FAT carboxyl-terminal domain that may regulate protein activity and stability (Perry and Kleckner, 2003). ATM activation requires functional NBS1 (Cerosaletti and Concannon, 2004; Difilippantonio et al., 2005; Falck et al., 2005; Cerosaletti et al., 2006). Mutations in the *NBS1* gene are responsible for Nijmegen breakage syndrome (NBS), a hereditary disorder that imparts an increased predisposition to development of malignancy and a hypersensitivity to IR (Shiloh, 1997). NBS1 forms a complex with Mre11 and Rad50 to be called the MRN complex. MRN is highly conserved, and it influences each aspect of chromosome break metabolism (Varon et al., 1998). Studies have shown that the MRN complex can detect DNA double-strand breaks and recruit ATM to damaged DNA molecules (Lee and Paull, 2004, 2005). The C terminus motif of NBS1 contains a conserved sequence motif that binds to two of the HEAT repeats (2 and 7) of ATM. This interaction is essential to activate the kinase (Falck et al., 2005).

Because the binding of NBS1 is critical for ATM to be functioning in response to DNA damage, we hypothesized that interfering with the NBS1-ATM interaction may block ATM activation and confer radiosensitization. To test this hypothesis, we developed several small peptides containing the conserved C-terminal sequence motif of NBS1 and fused them to a polyarginine internalization sequence. Herein, we describe the characterization of the C-terminal NBS1 inhibitory peptide in terms of internalization, half-life, cellular cytotoxicity, effects on the DNA damage response, and radiosensitivity. Together, these data may lead to a better understanding of the mechanisms that could be used to increase the radiosensitivity of cancer and provide data that could be rapidly translated into the development of novel radiosensitizing drugs.

## Materials and Methods

**Cell Culture.** Human tumor cell lines HeLa and DU-145 (American Type Culture Collection, Manassas, VA), and human simian virus-40 transformed fibroblast cell line GM9607 (Corriell Cell Repositories, Camden, NJ) were maintained in exponential growth in DMEM/10% FBS, in a 5% $CO_2$ humidified atmosphere. The glioma cell line M059J (Corriell Cell Repositories) were maintained in exponential growth in RPMI 1640 medium/15% FBS in a 5% $CO_2$ humidified atmosphere.

**Peptide Synthesis.** All peptides were synthesized by Abgent (San Diego, CA) and labeled with a biotin tag at their N termini for detection in vitro. Three peptides were produced: 1) one containing the polyarginine ($R_9$) internalization sequence alone, 2) a wild-type NBS1 inhibitory peptide (wtNIP) corresponding to amino acids 735 to 744 of human NBS1, and 3) a random sequence peptide in which amino acids 735 to 744 of human NBS1 were scrambled (scNIP). The peptides were dissolved in dimethyl sulfoxide, stored at −20°C, and reconstituted in DMEM/10% FBS before use.

**Irradiation.** An X-RAD 320 Irradiation Cabinet (Precision X-Ray, East Haven, CT) was employed at 320 kV and 160 mA, with a 0.8-mm Sn + 0.25-mm Cu + 1.5-mm Al (half-value layer ≅ 3.7 Cu) filter at a target-to-source distance of 20 cm and a dose rate of 3.4 Gy/min. All irradiations were conducted under normal atmospheric pressure and temperature.

**Immunoprecipitation and Western Blotting.** For coimmunoprecipitation of ATM, NBS1, and MRE11, cells were lysed for 1 h in ice-cold lysis buffer, which consisted of 10 mM Tris-HCl, pH 7.5, 100 mM NaCl, 5 mM EDTA, 0.5% Nonidet P-40, 5 mM $Na_3VO_4$, 1 mM NaF, and 1 mM phenylmethylsulfonyl fluoride. After centrifugation, supernatants were incubated with antibodies. After extensive washing with the lysis buffer, immunoprecipitates were analyzed by immunoblot using specific antibodies. For Western blotting analysis, samples (cell lysates or immunoprecipitates) were separated on to 2% SDS-polyacrylamide gels, transferred to nitrocellulose membranes, and probed with various antibodies.

**Immunofluorescence Microscopy.** Exponentially growing cultures of cells were plated on sterile 22-$cm^2$ coverslips and incubated for 24 h at 37°C in 5% $CO_2$ humidified air before they were treated with the NIP peptides at room temperature. Coverslips were washed with phosphate-buffered saline and fixed with 4% paraformaldehyde and 0.25% Triton X-100 for 15 min at room temperature, blocked for 30 min at room temperature, and incubated with fluorescein isothiocyanate-conjugated streptavidin or anti-γ H2AX and phospho-NBS1 antibodies (Rockland Immunochemicals, Gilbertsville, PA) for 1 h at room temperature. Coverslips were then mounted with Vectashield Elite (Vector Labs, Burlingame, CA) and observed with a Leica fluorescence microscope. Images were captured at 40× magnification using a Retiga EXi digital camera (QImaging, Surrey, BC, Canada) and analyzed with Image-Pro Plus software (ver. 4.1; Media Cybernetics, Inc., Bethesda, MD).

**MTT Assay.** For cytotoxicity studies, exponentially growing cultures of HeLa or DU-145 cells were harvested, plated in 96-well plates (5000 cells/well) in complete media, and incubated overnight. On the following day, cells were treated with the NIP peptides (0, 5, 10, 20, 50, or 100 μM) or paclitaxel (Taxol; 0, 10, 50 or 100 μM) as a positive control. At the end of the time course, an MTT cell viability assay (Promega Corp., Madison, WI) was used according to the manufacturer's guidelines to determine peptide cytotoxicity.

**Colony Formation Assays.** To determine radiosensitivity, the colony-forming assay was incorporated. Cells were harvested with 0.125% trypsin/0.05% EDTA, pelleted, and resuspended in 1 ml of fresh media with a 22-gauge needle to disperse clumps before hemocytometer counting in trypan blue. Cells were then plated at limiting dilutions in six-well plates and allowed to adhere overnight. Cultures were treated with phosphate-buffered saline, $R_9$, wtNIP, or scNIP for 1 h and irradiated (0–6Gy). Fresh peptides were added every 4 h until 24 h after IR, when the medium was replaced with peptide-free medium. Cultures were incubated for 1 to 2 days, harvested, and stained with 0.5% crystal violet in methanol. Colony number was determined with a dissecting microscope. A population of >50 cells was counted as one colony, and the number of colonies was expressed as a percentage of the value for untreated mock-irradiated control cells. The surviving curves were plotted by linear regression analyses, and the $D_0$ value represents the radiation dose that leads to 37% of survival. To determine the radiosensitizing potential of the peptides compared with other small-molecule inhibitors, we calculated the sensitizing enhancement ratio (SER) based on the dose of radiation required to reduce survival to 37% in the presence of scNIP or wtNIP. The following formula was used:

$$\text{SER} = \frac{D_0 \text{ for scNIP-treated cells}}{D_0 \text{ for wtNIP-treated cells}}$$

**Statistics.** To establish statistical significance, Student's $t$ test was incorporated. The data were first fit to each experimental group over a dose range of 0 to 6 Gy. Significant differences were established at $p < 0.05$.

## Results

**Internalization and Cytotoxicity of the C-Terminal NBS1 Inhibitory Peptides.** Previous studies have revealed that the C-terminal NBS1 domain is critical for its binding to ATM, and an NBS1 truncated derivative lacking the C-terminal 20 residues does not associate with ATM in vitro (Cerosaletti and Concannon, 2003, 2004; Falck et al., 2005; Cerosaletti et al., 2006). In addition, it has been shown that expression of an NBS1 transgene lacking the ATM binding domain in NBS cells leads to a dramatic reduction in ATM activation (Difilippantonio et al., 2005). Because inhibiting NBS1 association with ATM leads to suboptimal ATM activation after IR, the NBS1-ATM interaction can be a novel target for developing radiosensitizers. One approach to inhibiting NBS1-ATM interaction would be to use small peptides containing the conserved C-terminal sequence,which will presumably compete with endogenous NBS1-ATM interactions (Fig. 1A). Therefore, we designed peptides containing two functional domains: one an interfering domain that will inhibit the NBS1-ATM association, and the other an internalization domain that will transport the interfering peptides into cells. For the interfering domain, we used the amino acid sequences containing the conserved C-terminal motif of NBS1 as shown in Fig. 1B. This sequence contains the shortest ATM binding motif based on in vitro data (data not shown). For the internalization domain, we used a polyarginine sequence, which has been shown to have a significant efficiency of transporting small peptides and proteins across the plasma membrane (Fuchs and Raines, 2004; Deshayes et al., 2005) Three peptides were generated, including the $R_9$-alone, and a wtNIP corresponding to amino acids 73to 44 of human NBS1. The third peptide was designed as a negative control, using a random sequence generator to produce a peptide in which amino acids 735 to 744 of NBS1 were scrambled (scNIP). These peptides were labeled with a biotin tag at their N termini for detection in vitro.

We first evaluated the internalization of the fusion peptides. Treatment of HeLa cells with $R_9$, wtNIP, or scNIP at a concentration of 10 $\mu$M for 1 h led to a significant cellular uptake of peptide (Fig. 2). $R_9$, wtNIP, and scNIP internalization was localized to the cytoplasmic and nuclear compartments, whereas the control group, treated with DMEM alone, shows no fluorescent signal. Because the peptides would be used in radiation studies, we then determined the length of time the peptides remain in cells to ensure that the peptides would be present throughout the DNA repair process after IR. Cells treated with wtNIP or scNIP have significantly decreased fluorescence 8 h after treatment (Supplemental

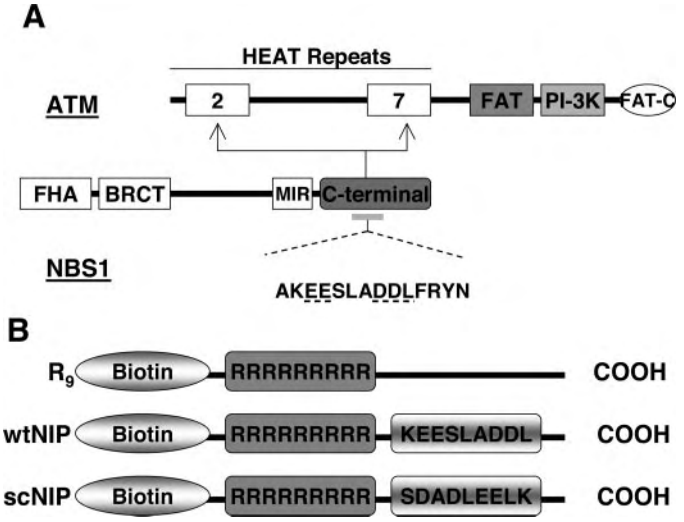


**Fig. 1.** Development of the NBS1 inhibitory peptides. A, schematic illustration of functional domains of ATM and NBS1 and their interaction. The C terminus of NBS1 is required for ATM activation and recruitment to sites of DNA damage. It consists of at least two sets of amino acid residues, 736 to 737 (EE) and 741 to 742 (DDL), that are evolutionarily conserved and necessary for ATM binding. NBS1 binds to two sets of the HEAT repeats [HEAT repeat 2 (amino acids 248–522) and HEAT repeat 7 (amino acids 1436–1770)] in ATM. B, the amino acid sequences for the $R_9$, wtNIP, and scNIP peptides developed.

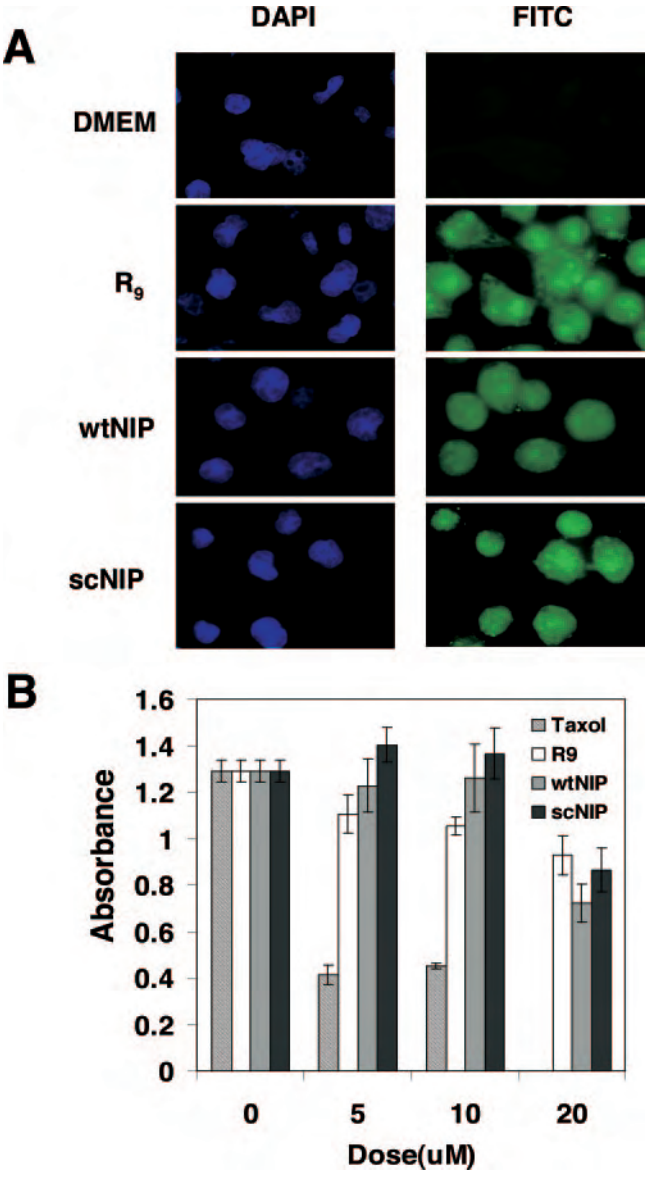


**Fig. 2.** Peptide internalization and cytotoxicity. A, HeLa cells were treated with 10 $\mu$M $R_9$, wtNIP, or scNIP for 1 h and analyzed by immunofluorescence microscopy after staining with fluorescein-conjugated streptavidin. B, HeLa cells were treated with paclitaxel and the NIP peptides at indicated doses. Twenty-four hours after treatment, cell survival was quantified by a standard MTT assay.

Fig. 1), suggesting that the NIP peptides should be added to cells every 4 to 6 h in the first 24 h after treatment with IR to achieve maximum inhibitory effects.

We then determined in vitro cytotoxicity of $R_9$, wtNIP and scNIP. HeLa cells grown in 96-well plates were treated with the peptides (0, 5, 10, 20, 50, or 100 $\mu$M) or paclitaxel (0, 10, 20, 50, or 100 $\mu$M) for 24 h. After treatment, the MTT assay was used to measure the production of solubilized formazan, a metabolic indicator of cell proliferation. The peptides demonstrated no growth inhibitory or cytotoxic effects up to 72 h after treatment (Fig. 2B), when the peptide doses were lower than 20 $\mu$M. Based on the cytotoxicity observed in the MTT assay, we chose 10 $\mu$M as the working concentration for all subsequent experiments. The effect of 10 $\mu$M $R_9$, wtNIP, and scNIP on clonogenic survival displayed no significant difference between treatment groups ($p < 0.05$) (Data not shown). It is noteworthy that dose and time course experiments have been preformed in several other cell lines, and our data confirmed rapid internalization and minimal cytotoxicity of these peptides (data not shown).

**wtNIP Abrogated the NBS1-ATM Interaction.** To investigate whether $R_9$-conjugated NIP peptides could inhibit NBS1-ATM interactions, we performed coimmunoprecipitation experiments in cells treated with the NIP peptides. Four hours after peptide treatment, HeLa cells were harvested and subjected to immunoprecipitation using an anti-NBS1 antibody. The immunoprecipitates were then blotted with anti-ATM, NBS1, and MRE11 antibodies. We observed a normal level of ATM-NBS1 association in $R_9$-treated cells compared with control cells. However, in wtNIP-treated cells, NBS1 was no longer able to bring down ATM (Fig. 3). Furthermore, the wtNIP affected only the NBS1-ATM interaction and did not interfere with NBS1 binding to MRE11. In contrast, scNIP did not affect the NBS1-ATM interaction. In cells treated with IR, wtNIP showed an effect similar to that in unirradiated cells. These observations demonstrate that wtNIP can abrogate the NBS1-ATM interaction in the absence or the presence of DNA damage.

**wtNIP Inhibits IR-Induced γ-H2AX and NBS1 pSer343 Focus Formation.** One of the earliest responses to IR-induced DNA damage is the formation of γ-H2AX foci, which requires functional ATM (Burma et al., 2001; Furuta et al., 2003). Because wtNIP showed an inhibitory effect on the NBS1-ATM interaction, we investigated whether IR-induced γ-H2AX focus formation was inhibited by the peptide. Immunofluorescence microscopy was used to detect the presence of γ-H2AX foci in mock-irradiated or irradiated cells in the presence of $R_9$, wtNIP or scNIP. The average number of γ-H2AX foci/nucleus in HeLa cells significantly increased after IR in cells treated with $R_9$ (42 foci/nucleus) or scNIP (41 foci/nucleus), whereas cells treated with wtNIP displayed only an average of 6.9 γ-H2AX foci/nucleus, similar to that of mock-irradiated cells (Fig. 4). Similar results were observed in DU-145 cells, whereas $R_9$ or scNIP exposure did not affect IR-induced focus formation, and wtNIP showed significantly reduced H2AX foci/nucleus (Supplemental Fig. 2). Therefore, IR-induced γ-H2AX focus formation can be inhibited by wtNIP.

To further support the idea that wtNIP can inhibit ATM-mediated DNA damage pathways, we investigated IR-induced NBS1 focus formation, an event considered to be an ATM-dependent process at the sites of DSBs (Lim et al., 2000). NBS1 foci are a result of ATM-mediated NBS1 phosphorylation on serine 343. Using an anti-phospho-Ser343 NBS1 antibody, we observed that NBS1 phosphorylation was significantly inhibited in cells treated with wtNIP compared with those treated with $R_9$ or scNIP (Fig. 5A and supplemen-

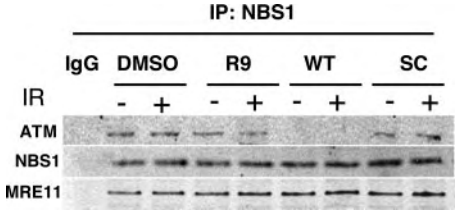


**Fig. 3.** wtNIP inhibits NBS1-ATM binding. HeLa cells treated with the NIP peptides were irradiated (0 or 6 Gy). Immunoprecipitation was performed with a rabbit NBS1 antibody, and Western blotting was performed with monoclonal antibodies against ATM, NBS1, or MRE11.

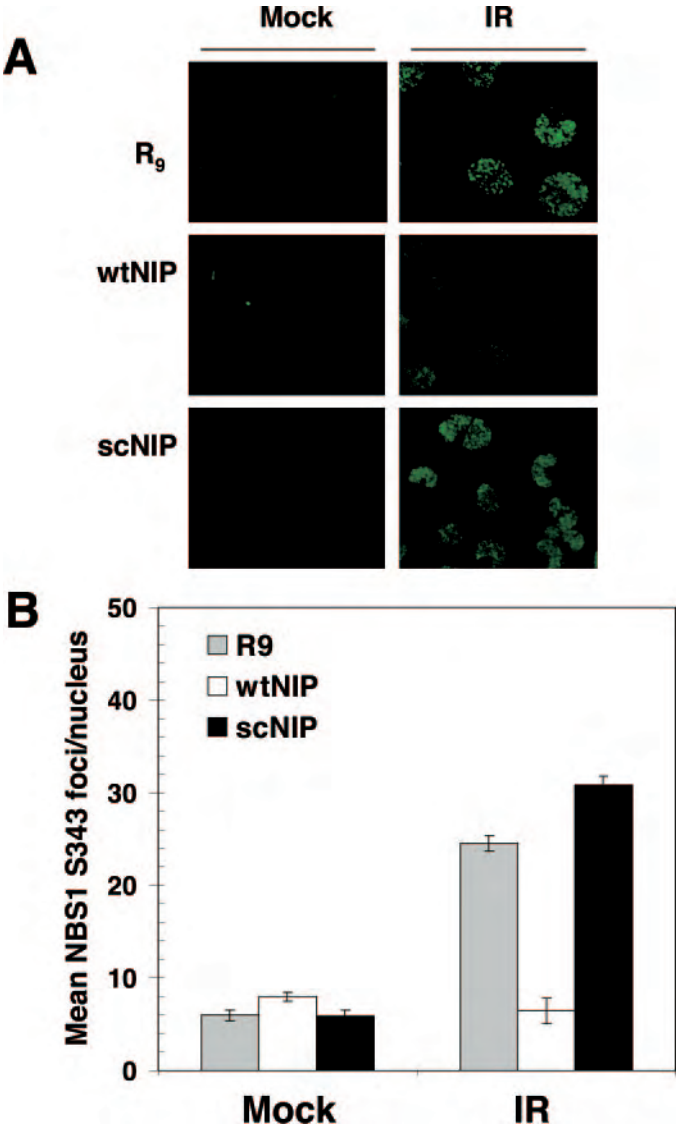


**Fig. 4.** WtNIP can inhibit γ-H2AX focus formation. A, HeLa cells were treated with 10 $\mu$M $R_9$, wtNIP, or scNIP for 1 h, irradiated with 0 or 6Gy, and harvested 30 min later before immunofluorescence microscopy was employed to detect radiation induced-γ -H2AX foci. B, the mean γ-H2AX nuclear foci per nucleus were determined for each image using Image-Pro Plus 5.1 software and is expressed in arbitrary units. Error bars represent ± 1 S.D.; graphed are the mean of three independent experiments.

tal Fig. 3A). The average number of foci in mock-irradiated HeLa cells was 6, 8, and 6 for $R_9$, wtNIP, and scNIP, respectively. Cells treated with $R_9$ or scNIP displayed 25 and 31 foci per nucleus, whereas cells treated with wtNIP showed only 6 foci per nucleus after treatment with 6-Gy IR (Fig. 5B).

It is important to note that there was a low level of background focus formation for both NBS1 and γ-H2AX phosphorylation, which has been correlated to mitosis in normally growing mammalian cell cultures (McManus and Hendzel, 2005).

**wtNIP Increases Radiation Sensitivity.** We then tested whether exposure to the NIP peptides will increase cellular radiosensitivity using the colony forming assay. Figure 6A depicts the survival curves for HeLa cells treated with $R_9$, wtNIP, or scNIP over a dose range of 0 to 6 Gy. We found that neither $R_9$ nor scNIP affects radiosensitivity, whereas wtNIP can significantly decrease IR-induced survival. Radiation survival curves were characterized based on $D_0$ to define the effect of NIP effect on radiosensitivity. $D_0$ represents the mean lethal dose required for 37% survival and is a measure of the intrinsic radiosensitivity of the cell. $D_0$ values for HeLa treated with wtNIP were 1.9 compared with 3.0 for cells treated with scNIP. To establish the statistical significance of wtNIP-induced radiosensitivity, Student's *t* test (paired two-sample for means) was incorporated. The data were first fit to each experimental group over a dose range of 0 to 6 Gy. Significant differences ($p < 0.05$) in clonogenic survival were observed between cells treated with wtNIP and those treated with DMEM, $R_9$, or scNIP. The SER was 1.58. This is comparable with other tested radiosensitizers, including gemcitabine, 5-fluorouracil, pentoxifylline, vinorelbine, and some ATM-specific radiosensitizers with SERs from 1.1 to 2.5 (Zhang et al., 1998; Lawrence et al., 2001; Robinson and Shewach, 2001; Strunz et al., 2002; Collis et al., 2003; Zhang et al., 2004). These observations have been confirmed in the prostate cancer cell line DU-145 (data not shown) with an SER of 1.46. Taken as a whole , they provide strong evidence for the radiosensitizing potential of the wtNIP peptide.

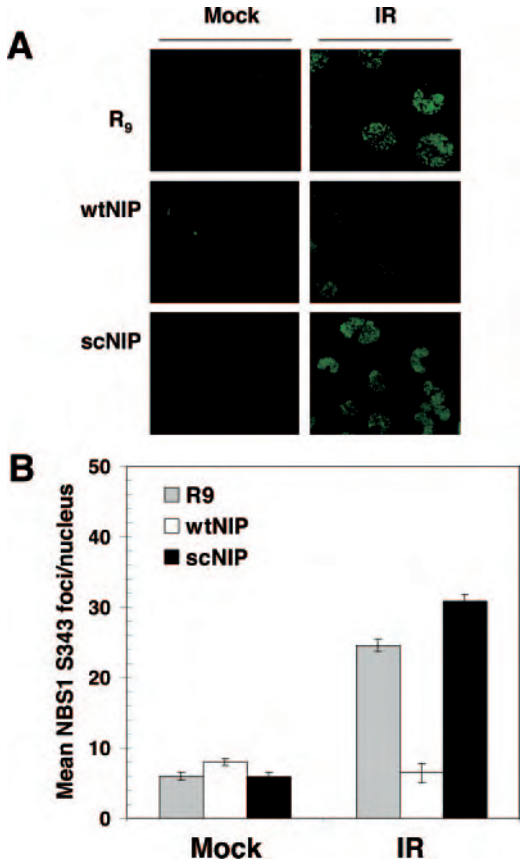


**Fig. 5.** Exposure to the wtNIP peptide abrogates IR-induced NBS1 phosphorylation. A, HeLa cells were treated with 10 μM $R_9$, wtNIP, or scNIP for 1 h, irradiated with 0 or 6Gy, and harvested 120 min later before immunofluorescence microscopy was employed to detect radiation induced-NBS1 focus formation using an anti-Ser343 NBS1 antibody. B, the mean number of NBS1 foci per nucleus was determined from a population of at least 25 cells in three independent experiments. Error bars represent ± 1 S.D.; graphed are the mean of three independent experiments.

Because wtNIP contains the conserved ATM binding sequence of NBS1, and this sequence is also conserved in the C terminus of ATR-interacting protein and KU80, the interacting proteins of ATR and DNA-PKcs, respectively, it was possible that it might also inhibit ATR or DNA-PKcs (Abraham, 2001). To test this possibility, we performed colony-forming assays in cell lines with defective ATM (GM9607) or DNA-PKcs (M059J). Although treatment with wtNIP led to an increase in radiosensitivity in M059J cells (Fig. 6C) with an SER of 1.83, GM9607 (Fig. 6D) displayed no change in radiosensitivity. Because GM9607 cells are ATM-deficient and have functional ATR and DNA-PKcs, our observations strongly suggest that wtNIP can specifically target ATM, but not ATR or DNA-PKcs, to achieve radiosensitization.

## Discussion

Because ATM is central to cellular responses to irradiation, blocking its activation or activity could make any type of tumor much more sensitive to radiation. Since cloning the gene in 1995, investigators have employed several methods to develop specific ATM inhibitors. These methods include antisense RNA, small interfering RNA (siRNA), and screening of small molecule inhibitors of ATM. Subcloning a full-length cDNA of ATM in the opposite orientation into CB3AR cells significantly increased radiosensitivity (Zhang et al., 1998). The development of siRNA also led to the generation of an siRNA that could inhibit ATM function in prostate cancer cells. Both DU-145 and PC-3 cells, when transfected with these plasmids, exhibited an increase in radiosensitivity at clinically relevant radiation doses (Collis et al., 2003). More recently, the use of high-throughput screening has provided a new generation of ATM inhibitors that can be quickly translated to clinical studies. By screening a combinatorial library of compounds around the DNA-PKcs inhibitor LY294002, Hickson et al. (2004) reported a compound (KU55933) to selectively inhibit the ATM kinase. Their studies have shown a significant increase in radiosensitivity in HeLa cells. However, the in vivo radiosensitization effect and the toxicity of the compounds have not been reported.

Despite these promising findings, one of the major concerns of developing ATM inhibitors is the uncertainty of pleiotropic effects of such inhibitors. Due to the complex effects associated with malfunction of the protein kinase, the outcome of directly targeting ATM kinase activity can be complicated, in that it is unclear whether the only effect of these reagents will be to confer radiosensitization.

Instead of directly inhibiting the ATM kinase activity to

increase radiosensitivity, an alternative approach is to target IR-induced ATM activation, because this will directly lead to an increase in radiosensitivity without interfering with other important functions of ATM in the absence of DNA damage. Because the NBS1-ATM interaction is important for IR-induced activation of ATM, selectively disrupting the signaling pathway would be a novel approach for developing radiosensitizers. Furthermore, because the C-terminal of NBS1 association with ATM is necessary for ATM activation, we reasoned that a small peptide containing a portion of this conserved C-terminal domain (i.e., KEESLADDL) would compete with the NBS1-ATM association in vivo and sensitize tumor cells to radiation. Our data demonstrate that the wild-type NBS1 peptide can be used to inhibit ATM activation and induce radiosensitization.

Because the wtNIP peptide contains the conserved sequence among the phosphatidylinositol 3-kinase interacting proteins, such as ATR-interacting protein and Ku80 (Falck et al., 2005), we further reasoned that wtNIP could possibly interfere with ATR and DNA-PKcs activation. We tested the radiosensitizing effect of the peptides in cells with deficient ATM or DNA-PKcs. If the wtNIP could inhibit ATR or DNA-PKcs, then the ATM-deficient cells should be sensitized. However, the radiosensitivity of GM9607, which lacks ATM but has functional ATR and DNA-PKcs, was not affected by the peptide. In contrast, the DNA-PKcs mutant cells showed an increased radiosensitivity similar to that of HeLa and DU-145 cells treated with wtNIP. These observations therefore demonstrate specific ATM inhibition by the wtNIP peptide.

In summary, we have established a proof of principle in vitro, with results that may lend insight into a novel approach to the development of powerful radiosensitizers for clinical cancer therapy and use the peptides as specific ATM

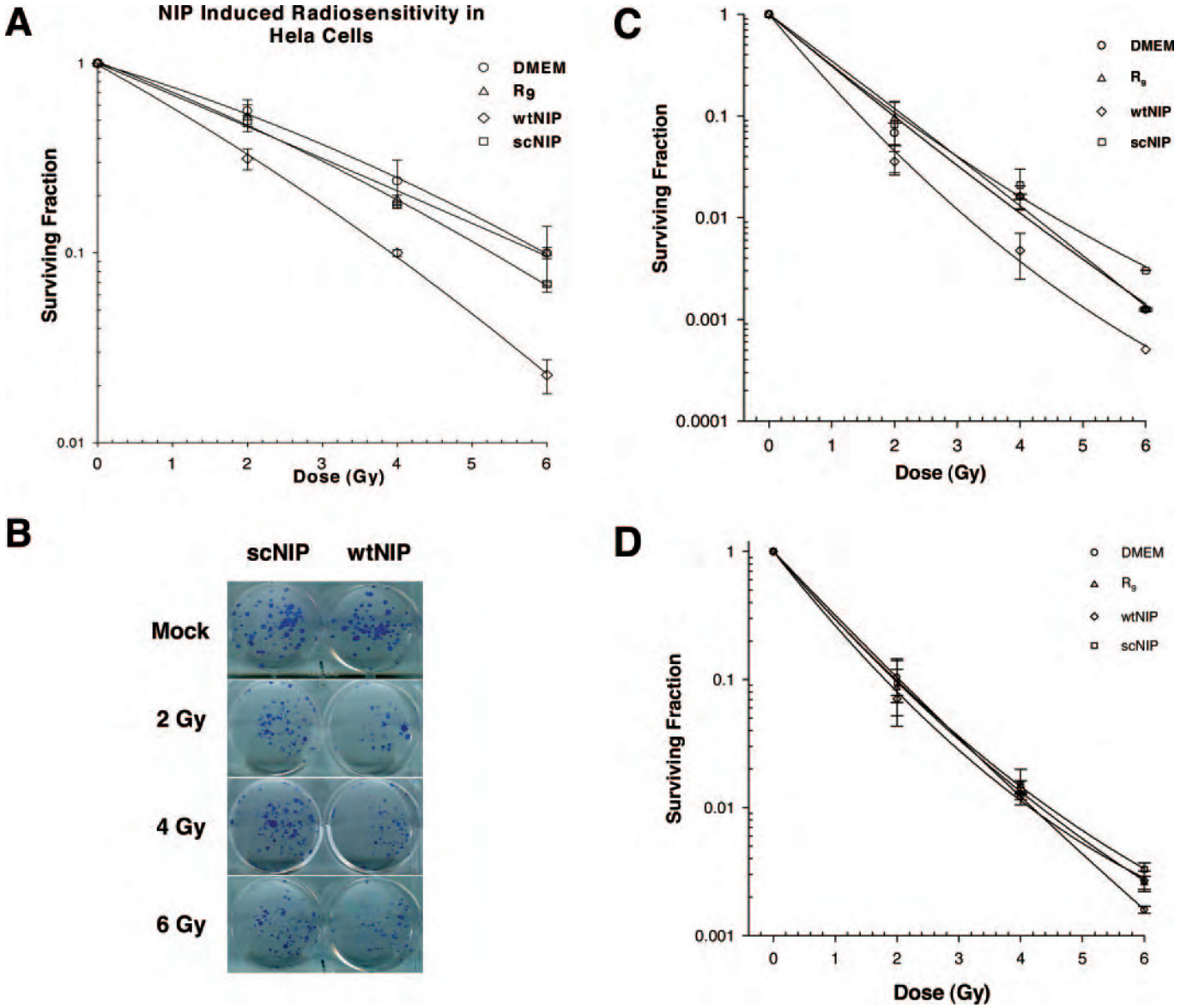


**Fig. 6.** WtNIP increases cellular radiosensitivity. Cells were seeded at limiting dilutions and treated with 10 $\mu$M $R_9$, wtNIP, or scNIP for 1 h before irradiation, continuously exposed to the peptides for 24 h, harvested 10 to 12 days later, and stained with crystal violet. Shown in A (HeLa), C (MO59J), and D (GM9607) are the surviving curves after indicated doses of radiation. Error bars represent ± 1 S.E.M.; graphed are the mean of three independent experiments. B, representative plates of the clonogenic assay for NIP-mediated radiosensitivity in HeLa cells.

inhibitors for further elucidation of signaling pathways involved in the DNA damage response. However, the use of the polyarginine-mediated NBS1 peptide as a therapeutic agent still faces challenges such as peptide stability, toxicity, tumor specific targeting, and immunogenic effects, etc. Using the current concept to establish an assay for high-throughput screening to identify small molecules that can target the NBS1-ATM interaction will eventually lead to novel radiosensitizers usable for clinical settings. Future studies are also necessary to determine the structure of the NBS1-ATM interaction complex and how wtNIP competes with the interaction.

**Acknowledgments**

We thank all members in the Xu lab for the technical help.

**References**

Abraham RT (2001) Cell cycle checkpoint signaling through the ATM and ATR kinases. *Genes Dev* **15:**2177–2196.

Burma S, Chen BP, Murphy M, Kurimasa A, and Chen DJ (2001) ATM phosphorylates histone H2AX in response to DNA double-strand breaks. *J Biol Chem* **276:**42462–42467.

Cerosaletti K and Concannon P (2004) Independent roles for nibrin and Mre11-Rad50 in the activation and function of Atm. *J Biol Chem* **279:**38813–38819.

Cerosaletti K, Wright J, and Concannon P (2006) Active role for nibrin in the kinetics of atm activation. *Mol Cell Biol* **26:**1691–1699.

Cerosaletti KM and Concannon P (2003) Nibrin forkhead-associated domain and breast cancer C-terminal domain are both required for nuclear focus formation and phosphorylation. *J Biol Chem* **278:**21944–21951.

Collis SJ, Swartz MJ, Nelson WG, and DeWeese TL (2003) Enhanced radiation and chemotherapy-mediated cell killing of human cancer cells by small inhibitory RNA silencing of DNA repair factors. *Cancer Res* **63:**1550–1554.

Deshayes S, Morris MC, Divita G, and Heitz F (2005) Cell-penetrating peptides: tools for intracellular delivery of therapeutics. *Cell Mol Life Sci* **62:**1839–1849.

Difilippantonio S, Celeste A, Fernandez-Capetillo O, Chen HT, Reina SM, Van Laethem F, Yang YP, Petukhova GV, Eckhaus M, Feigenbaum L, et al. (2005) Role of Nbs1 in the activation of the Atm kinase revealed in humanized mouse models. *Nat Cell Biol* **7:**675–685.

Falck J, Coates J, and Jackson SP (2005) Conserved modes of recruitment of ATM, ATR and DNA-PKcs to sites of DNA damage. *Nature* **434:**605–611.

Fuchs SM and Raines RT (2004) Pathway for polyarginine entry into mammalian cells. *Biochemistry* **43:**2438–2444.

Furuta T, Takemura H, Liao ZY, Aune GJ, Redon C, Sedelnikova OA, Pilch DR, Rogakou EP, Celeste A, Chen HT, et al. (2003) Phosphorylation of histone H2AX and activation of Mre11, Rad50, and Nbs1 in response to replication-dependent DNA double-strand breaks induced by mammalian DNA topoisomerase I cleavage complexes. *J Biol Chem* **278:**20303–20312.

Hickson I, Zhao Y, Richardson CJ, Green SJ, Martin NM, Orr AI, Reaper PM, Jackson SP, Curtin NJ, and Smith GC (2004) Identification and characterization of a novel and specific inhibitor of the ataxia-telangiectasia mutated kinase ATM. *Cancer Res* **64:**9152–9159.

Lawrence TS, Davis MA, Hough A, and Rehemtulla A (2001) The role of apoptosis in 2′,2′-difluoro-2′-deoxycytidine (gemcitabine)-mediated radiosensitization. *Clin Cancer Res* **7:**314–319.

Lee JH and Paull TT (2004) Direct activation of the ATM protein kinase by the Mre11/Rad50/Nbs1 complex. *Science* **304:**93–96.

Lee JH and Paull TT (2005) ATM activation by DNA double-strand breaks through the Mre11-Rad50-Nbs1 complex. *Science* **308:**551–554.

Lim DS, Kim ST, Xu B, Maser RS, Lin J, Petrini JHJ, and Kastan MB (2000) ATM phosphorylates P95/Nbs1 in an S-phase checkpoint pathway. *Nature* **404:**613–617.

McManus KJ, and Hendzel MJ (2005) ATM-dependent DNA damage-independent mitotic phosphorylation of H2AX in normally growing mammalian cells. *Mol Biol Cell* **16:**5013–5025.

Perry J and Kleckner N (2003) The ATRs, ATMs, and TORs are giant HEAT repeat proteins. *Cell* **112:**151–155.

Robinson BW and Shewach DS (2001) Radiosensitization by gemcitabine in p53 wild-type and mutant MCF-7 breast carcinoma cell lines. *Clin Cancer Res* **7:**2581–2589.

Shiloh Y (1997) Ataxia-telangiectasia and the nijmegen breakage syndrome: related disorders but genes apart. *Annu Rev Genet* **31:**635–662.

Shiloh Y (2003) ATM and related protein kinases: safeguarding genome integrity. *Nat Rev Cancer* **3:**155–168.

Strunz AM, Peschke P, Waldeck W, Ehemann V, Kissel M, and Debus J (2002) Preferential radiosensitization in p53-mutated human tumour cell lines by pentoxifylline-mediated disruption of the g2/m checkpoint control. *Int J Radiat Biol* **78:**721–732.

Varon R, Vissinga C, Platzer M, Cerosaletti KM, Chrzanowska KH, Saar K, Beckmann G, Seemanova E, Cooper PR, Nowak NJ, et al. (1998) Nibrin, a novel DNA double-strand break repair protein, is mutated in Nijmegen breakage syndrome. *Cell* **93:**467–476.

Zhang M, Boyer M, Rivory L, Hong A, Clarke S, Stevens G, and Fife K (2004) Radiosensitization of vinorelbine and gemcitabine in NCI-H460 non-small-cell lung cancer cells. *Int J Radiat Oncol Biol Phys* **58:**353–360.

Zhang N, Chen P, Gatei M, Scott S, Khanna KK, and Lavin MF (1998) An anti-sense construct of full-length ATM CDNA imposes a radiosensitive phenotype on normal cells. *Oncogene* **17:**811–818.

**Address correspondence to:** Bo Xu, MD, PhD, Southern Research Institute, Department of Biochemistry and Molecular Biology, 2000 9th Avenue South, Birmingham, AL 35205. E-mail: xu@sri.org 32

MOLECULAR AND CELLULAR BIOLOGY, Apr. 2008, p. 2559–2566 Vol. 28, No. 8
0270-7306/08/$08.00+0 doi:10.1128/MCB.01711-07


# A Novel ATM-Dependent Pathway Regulates Protein Phosphatase 1 in Response to DNA Damage▽†

Xi Tang,[1,2] Zhou-guang Hui,[2] Xiao-li Cui,[1] Renu Garg,[2] Michael B. Kastan,[3] and Bo Xu[1]*

*Department of Biochemistry and Molecular Biology, Southern Research Institute, and Department of Biochemistry and Molecular Genetics and Comprehensive Cancer Center, The University of Alabama at Birmingham, Birmingham, Alabama 35205[1]; Department of Genetics, Louisiana State University Health Sciences Center, New Orleans, Louisiana 70112[2]; and Department of Oncology, St. Jude Children's Research Hospital, Memphis, Tennessee 38105[3]*

Received 17 September 2007/Returned for modification 17 October 2007/Accepted 22 January 2008

**Protein phosphatase 1 (PP1), a major protein phosphatase important for a variety of cellular responses, is activated in response to ionizing irradiation (IR)-induced DNA damage. Here, we report that IR induces the rapid dissociation of PP1 from its regulatory subunit inhibitor-2 (I-2) and that the process requires ataxia-telangiectasia mutated (ATM), a protein kinase central to DNA damage responses. In response to IR, ATM phosphorylates I-2 on serine 43, leading to the dissociation of the PP1–I-2 complex and the activation of PP1. Furthermore, ATM-mediated I-2 phosphorylation results in the inhibition of the Aurora-B kinase, the down-regulation of histone H3 serine 10 phosphorylation, and the activation of the $G_2$/M checkpoint. Collectively, the results of these studies demonstrate a novel pathway that links ATM, PP1, and I-2 in the cellular response to DNA damage.**

Optimal cellular responses to DNA damage are mediated by protein kinases and phosphatases in order to promote survival and limit genetic instability. The *a*taxia-*t*elangiectasia *m*utated kinase, ATM, plays a crucial role in the cellular response to DNA damage. The loss of ATM functions in humans results in progressive neurodegeneration, immunodeficiency, glucose intolerance, sterility, predisposition to lymphoblastoid malignancies, and radiation sensitivity (25). Cellular phenotypes of ATM deficiency include suboptimal activation of radiation-induced cell cycle checkpoints, increased spontaneous and DNA damage-induced chromosomal breakage and gaps, and hypersensitivity to radiation, etc. Human ATM is a 3,056-amino-acid polypeptide which shares several features with other members of the phosphatidylinositol 3-kinase-like kinase family, including a FAT (FRAP, ATR, and TRRAP) domain, a phosphatidylinositol 3-kinase domain, and a FAT carboxyl-terminal domain (14). ATM, like other members of this protein kinase family, phosphorylates its substrates on serines or threonines that are followed by glutamine (the SQ or TQ motif) (12, 22). A number of downstream targets have been identified. These substrates include many tumor suppressors, such as p53, Brca1, and Chk2, and the functional significance of ATM phosphorylation has been studied previously. For example, in response to ionizing radiation (IR), ATM phosphorylates BRCA1 (at Ser 1387) (32), CHK2 (at Thr 68) (7), FANCD2 (at Ser 222) (27), NBS1 (at Ser 278 and Ser 343), and SMC1 (at Ser 957 and Ser 966) (13, 33) to facilitate the S-phase checkpoint. Large-scale proteomic analyses of proteins phosphorylated on the ATM and ATR consensus sites in response to DNA damage have identified more than 900 regulated phosphorylation sites encompassing over 700 proteins. Functional analyses of a subset of this data set have indicated that this list is highly enriched with proteins involved in the DNA damage response (17).

Protein serine/threonine phosphatases, which in humans include protein phosphatase 1 (PP1), PP2A, PP2B, PP4, PP5, PP6, and PP7, function by reversing the phosphorylation of key structural and regulatory proteins (3, 4). In this family, PP2A and PP5 have been reported previously to regulate ATM serine 1981 autophosphorylation after DNA damage (2, 8, 34). It has also been reported previously that PP1 is activated in an ATM-dependent manner in response to DNA damage (9). However, how ATM activates PP1, as well as the physiological function of ATM-mediated PP1 activation in the DNA damage response, remains unknown.

PP1 interacts with its regulatory subunits in controlling the specificity and diversity of the phosphatase function (3). Inhibitor-2 (I-2), a 23-kDa phosphoprotein, is a well-documented PP1 regulatory subunit. I-2 was originally isolated as a heat-stable protein from skeletal muscle extracts that could specifically inhibit PP1 activity (11). PP1 forms a stable and inactive complex with unphosphorylated I-2, and the activation of the complex is accompanied by the phosphorylation of I-2 (21). One established model is that glycogen synthase kinase 3 (GSK-3)-mediated threonine 72 phosphorylation of I-2 promotes a conformational change in the PP1–I-2 complex (1, 16). I-2 can be phosphorylated on other serine sites by casein kinase I (CKI) and CKII, cdc2, and mitogen-activated protein kinases (15, 29). Though phosphorylation by CKII does not alter I-2 activity, it greatly facilitates the subsequent phosphorylation by GSK-3 (3). Previous deletion and mutagenesis studies have demonstrated that the N-terminal domain of I-2 interacts with

* Corresponding author. Mailing address: Department of Biochemistry and Molecular Biology, Southern Research Institute, 2000 9th Ave. South, Birmingham, AL 35205. Phone: (205) 581-2845. Fax: (205) 581-2097. E-mail: xu@sri.org.

† Supplemental material for this article may be found at http://mcb.asm.org/.

▽ Published ahead of print on 4 February 2008.

PP1 (23) and can be dephosphorylated by PP1. Despite these findings, it is not known whether the PP1–I-2 complex is involved in DNA damage responses.

To study the mechanism of ATM-mediated PP1 activation, we investigated the IR-induced dissociation of the PP1–I-2 complex. We report here that the activation of PP1 is governed by ATM phosphorylation of I-2 at serine 43 in response to DNA damage and that ATM-mediated PP1 activation leads to the activation of the $G_2$/M checkpoint through the inhibition of the Aurora-B kinase.

## MATERIALS AND METHODS

**Cell culture.** Human cells lines 293T and HeLa (from the American Type Culture Collection, Manassas, VA), simian virus 40 (SV40)-transformed human fibroblast cell lines GM0637 and GM9607 (from the NIGMS Human Mutant Cell Repository, Camden, NJ), and SV40-transformed fibroblast cell lines PEB-vector and PEB-YZ5 (32) were grown as monolayers in Dulbecco's modified Eagle medium with high glucose levels. The cell culture medium was supplemented with 10% fetal bovine serum and 1% penicillin and 1% streptomycin. Epstein-Barr virus (EBV)-immortalized lymphoblastoid cell lines from healthy persons (GM0536; NIGMS) and from persons who were homozygous for the ATM mutation (GM1526) were cultured in RPMI 1640 supplemented with 15% fetal bovine serum. All cells were maintained in a humid incubator at 5% $CO_2$ and 37°C.

**Irradiation.** For irradiation treatments, an X-RAD 320 irradiation cabinet (Precision X-Ray, East Haven, CT) was utilized at 320 kV and 160 mA, with a 0.8-mm Sn, 0.25-mm Cu, 1.5-mm Al (half-value layer at 3.7 mm Cu) filter at a target-source distance of 20 cm and a dose rate of 3.4 Gy/min. All irradiation treatments were conducted under normal atmospheric pressure and at room temperatures.

**Antibodies.** Rabbit polyclonal antibodies against PP1 and phospho-histone H3 phosphorylated at serine 10 were purchased from Upstate Biotechnology (Temecula, CA). A rabbit polyclonal phospho-histone H1 antibody was obtained from Abcam (Cambridge, MA). A rabbit polyclonal antibody against I-2 was purchased from Calbiochem (San Diego, CA). Mouse anti-Flag antibodies M2 and M5 were obtained from Sigma-Aldrich (St. Louis, MO). The mouse anti-Xpress antibody was purchased from Invitrogen (Carlsbad, CA). The rabbit polyclonal antibody against phospho-Ser 43 of I-2 was generated through Alpha Diagnostic International (San Antonio, TX). Synthetic peptides representing the sequence surrounding serine 43 of I-2 and containing a phosphorylated serine linked with keyhole limpet hemocyanin at the site corresponding to serine 43 were generated. The immunogens were then injected into rabbits, and a polyclonal antibody was generated and purified.

**Plasmids.** Vectors that expressed glutathione *S*-transferase (GST)-conjugated I-2 and PP1 peptides were made by cloning complementary oligonucleotides that encoded the desired peptides (14 amino acids) into the BamHI-SmaI sites of pGEX-2T (Amersham Pharmacia Biotech, Piscataway, NJ). The QuikChange site-directed mutagenesis kit (Stratagene, Cedar, TX) was used to generate the serine-to-alanine mutant peptide. To construct Xpress-tagged I-2 expression vectors, we amplified the entire I-2 coding region by PCR with the following primers: 5′-CTGCGAGTCTCTGCTGTGCC-3′ and 5′-TGTGAAGAACAAG AAGCAACGTAC-3′. The PCR products were cloned into an Xpress-tagged pCDNA6 vector (Invitrogen, Carlsbad, CA) with the EcoRV restriction site. We then utilized the QuikChange site-directed mutagenesis kit to generate the serine-to-alanine mutant form. The oligonucleotides used for mutation were as follows: 5′-GAGCAAAAAAGCCCAGAAGTGG-3′ and 5′-CCACTTCTGGG CTTTTTTGCTC-3′.

**Nuclear and cytoplasmic fractionation.** Nuclear and cytoplasmic fractionation was carried out with a nuclear extraction kit (Chemicon, Temecula, CA), which was modified according to our experiments. Cells were collected with trypsinization and rinsed with ice-cold 1× phosphate-buffered saline (PBS) or 1× Tris-buffered saline. Then the sample was centrifuged at 250 × *g* for 5 min at 4°C. Cell pellets were resuspended with 10 cell pellet volumes of ice-cold 1× cytoplasmic lysis buffer containing 0.5 mM dithiothreitol and diluted protease inhibitor. The cell suspension was then centrifuged, and cell pellets were kept for resuspension with 5 volumes of ice-cold 1× cytoplasmic lysis buffer. The resuspended cells were disrupted using a syringe with a small-gauge needle (27 gauge), and the disrupted cell suspension was centrifuged at 8,000 × *g* for 20 min at 4°C. The supernatant contained the cytosolic portion of the cell lysates, while the remaining pellet contained the nuclear portion. The nuclear pellet was resuspended in a volume of ice-cold nuclear extraction buffer corresponding to two original cell pellet volumes and containing 0.5 mM dithiothreitol and diluted protease inhibitor. The nuclei were disrupted using a fresh syringe with a 27-gauge needle, and the nuclear suspension was gently agitated with an orbital shaker at 4°C for 1 h. The nuclear suspension was then centrifuged at 8,000 × *g* for 5 min at 4°C. The supernatant contained the nuclear portion of the cell lysates.

**Immunoprecipitation.** Cells were irradiated with 0 or 6 Gy, and the cell lysates were prepared as described in the previous section. The supernatants were incubated with anti-Flag M2, anti-Aurora-B, anti-PP1, or anti-Xpress antibodies. After extensive washing with the lysis buffer, immunoprecipitates were used for in vitro kinase assays or in vitro phosphatase assays or were analyzed by immunoblotting.

**In vitro kinase assays.** In vitro kinase assays for Flag-tagged ATM and Aurora-B were performed as described previously (12, 18). The immunoprecipitates were suspended in 50 μl of kinase buffer containing 10 μCi of [λ-$^{32}$P]ATP, 1 mM unlabeled ATP, and 1 μg of substrates (GST-conjugated peptides, recombinant I-2, or histone H3). The kinase reaction was conducted at 30°C for 30 min and stopped by the addition of sodium dodecyl sulfate-polyacrylamide gel electrophoresis loading buffer. The kinase assay products were separated by sodium dodecyl sulfate-polyacrylamide gel electrophoresis and transferred onto a nitrocellulose membrane. The phosphorylation signal was analyzed by autoradiography and quantified by a phosphorimager.

**In vitro phosphatase assays.** The in vitro phosphatase assays were performed using a Ser/Thr phosphatase assay kit (Upstate). Cytoplasmic, nuclear, or exogenous PP1 was immunoprecipitated, and the PP1 immune complex beads were incubated with a phosphopeptide (KRpTIRR, where p indicates the site of phosphorylation) at room temperature for 30 min. The beads were pelleted, and a 25-μl sample of the supernatant was analyzed for free phosphate in the malachite green assay by dilution with 100 μl of a developing solution (malachite green). After incubation for 15 min, the release of phosphate was quantified by measuring the absorbance at 650 nm in a microtiter plate reader.

**Histone H1 and H3 phosphorylation staining.** The histone H1 and H3 phosphorylation assay results were assessed as described previously (27, 29). Cells were harvested 90 min after IR, washed with PBS, and fixed in a suspension with 2 ml of 70% ethanol. After fixation, cells were washed twice with PBS, suspended in 1 ml of 0.15% Triton X-100 in PBS, and incubated on ice for 5 min. After centrifugation, the cell pellet was suspended in 100 μl of PBS containing 1% bovine serum albumin (BSA) and 0.75 μg of a polyclonal antibody that specifically recognized the phosphorylated form of histone H3 or H1 (Upstate or Abcam, Cambridge, MA, respectively) and the suspension was incubated for 3 h at room temperature. Then the cells were rinsed with PBS containing 1% BSA and incubated with fluorescein isothiocyanate-conjugated goat anti-rabbit immunoglobulin G antibody (Jackson ImmunoResearch Laboratories, West Grove, PA) diluted at a ratio of 1:30 in PBS containing 1% BSA. After a 30-min incubation at room temperature in the dark, the cells were washed again, resuspended in a mixture of 25 μg of propidium iodide/ml and 0.1 mg of RNase A (Sigma)/ml in PBS, and incubated at room temperature for 30 min before the fluorescence was measured. Cellular fluorescence was measured by using a Becton Dickinson FACSCalibur flow cytometer-cell sorter.

## RESULTS

**IR induces ATM-dependent dissociation of the PP1–I-2 complex.** In this study, we first confirmed that PP1 was activated in response to IR-induced DNA damage in an ATM-dependent manner (see Fig. S1A, C, and D in the supplemental material). We also found that only the nuclear fraction of PP1 was activated after IR and that the cytoplasmic fraction did not display IR-induced activation (see Fig. S1B in the supplemental material). Since PP1 is negatively regulated by I-2 in a variety of cellular events, it is possible that PP1 activation involves I-2. PP1 and I-2 form a complex to regulate PP1 activity; therefore, we explored the possibility of an alteration of the PP1–I-2 complex in response to DNA damage. The immunoprecipitation of PP1 from unirradiated cells brought down I-2, but following IR, I-2 was no longer detectable in the PP1 immunoprecipitates (Fig. 1A). We then tested the ATM dependency of this dissociation. While GM0637 cells (with functional ATM) had a noticeable dissociation of PP1–I-2 after

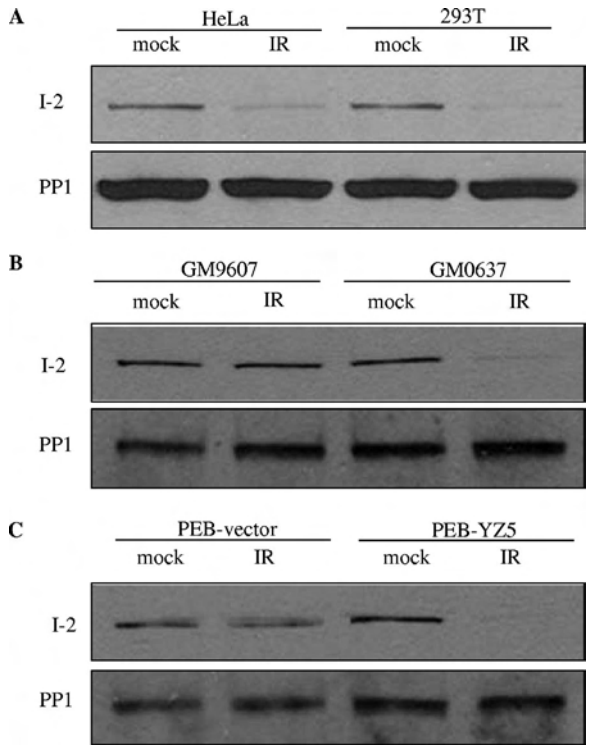


FIG. 1. The IR-induced dissociation of PP1 and I-2 requires functional ATM. Two hours after IR, immunoprecipitation from nuclear extracts was performed using an anti-PP1 antibody and immunoblot analyses were conducted using antibodies against I-2 or PP1 from HeLa and 293T cells (A), fibroblasts proficient (GM0637) or deficient (GM9607) in ATM (B), and isogenic fibroblasts deficient (PEB-vector) or proficient (PEB-YZ5) in ATM (C).

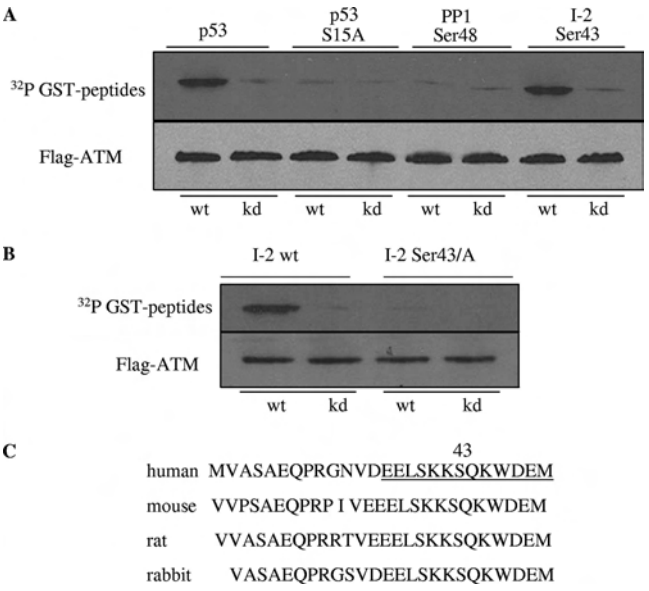


FIG. 2. ATM phosphorylates I-2 at serine 43 in vitro. (A) Immunoprecipitated Flag-tagged wild-type (wt) or kinase-dead (kd) ATM was incubated with recombinant proteins consisting of fusions between GST and peptides derived from various regions of human PP1 or I-2. The positions of the amino acids corresponding to each peptide are indicated at the top. p53 peptides (amino acids 1 to 101 for either the wild-type or the serine 15-to-alanine mutant form) were used as controls. (B) The full-length wild-type or serine 43-to-alanine mutant form of I-2 was used as the substrate for wild-type or kinase-dead ATM for the in vitro kinase assay. (C) Sequence homology of I-2 around serine 43 in different species. Underlining in the sequence from human I-2 indicates a sequence highly conserved among mammalian species.

IR, no detectable IR-induced PP1–I-2 dissociation occurred in GM9607 (ATM-deficient) cells (Fig. 1B). This phenotype was also observed in isogenic cell lines with an ATM deficiency (PEB-vector cells) and with reconstituted ATM (PEB-YZ5 cells) (Fig. 1C), demonstrating that ATM is required for the IR-induced PP1–I-2 dissociation.

**ATM phosphorylates I-2 at serine 43 in vitro.** Since the phosphorylation of the inhibitory subunit I-2 can activate PP1 (3), we wondered whether the direct phosphorylation of I-2 by ATM might lead to the activation of the phosphatase after IR. It was also possible that ATM could phosphorylate PP1 to activate it directly. To test these possibilities, we examined the ability of ATM to phosphorylate these substrates in vitro. A sequence search found that there was only one putative ATM target site (SQ or TQ) in PP1 (serine 48 and the adjacent glutamine) and one in I-2 (serine 43 and the adjacent glutamine). Recombinant GST fusion peptides containing amino acid sequences with these SQ sites were used as substrates for ATM in an in vitro kinase assay. GST-p53 (amino acids 1 to 101) and GST-p53 (amino acids 1 to 101 of the S15A mutant form) served as positive and negative substrate controls, respectively. A peptide containing serine 43 of I-2 exhibited a strong phosphorylation signal, while the phosphorylation of the PP1 serine 48 peptide was not above the background level (Fig. 2A). These observations suggested that serine 48 of PP1 was not likely to be a direct target of ATM but that serine 43 of I-2 was promising as a target. Progressing on to full-length I-2 protein as a substrate, we found that ATM phosphorylated wild-type I-2 but not I-2 with a serine 43-to-alanine mutation (Fig. 2B). Thus, serine 43 of I-2 appears to be an ATM target in vitro. It is noted that serine 43 and its surrounding residues are highly conserved among mammalian species (Fig. 2C).

**ATM phosphorylates I-2 at serine 43 in vivo after IR.** To better study the potential phosphorylation of I-2 in vivo, we generated an antibody that specifically recognizes I-2 serine 43 phosphorylation. The specificity of the phosphospecific antibody was demonstrated by its ability to recognize the phosphorylated, but not the unphosphorylated, peptide sequence (see Fig. S2 in the supplemental material). This antibody was used to probe for I-2 serine 43 phosphorylation in cells before and after IR. Several cell lines were tested, including HeLa and 293T cell lines, EBV-transformed lymphoblast cell lines with (GM 0536) and without (GM1526) ATM, and the isogenic cell lines PEB-vector (ATM null) and PEB-YZ5 (ATM complemented). Though total I-2 protein was easily detectable by Western blot analyses, with no notable changes before and after IR, no reactivity with the phosphoserine-specific antibody in unirradiated cells was seen. However, significant reactivity with the anti-phospho-serine 43 antibody in extracts from irradiated cells with functional ATM was observed (Fig. 3). No reactivity with the phosphoserine-specific antibody in ATM-deficient cells after IR was detected. Thus, ATM directly phos-

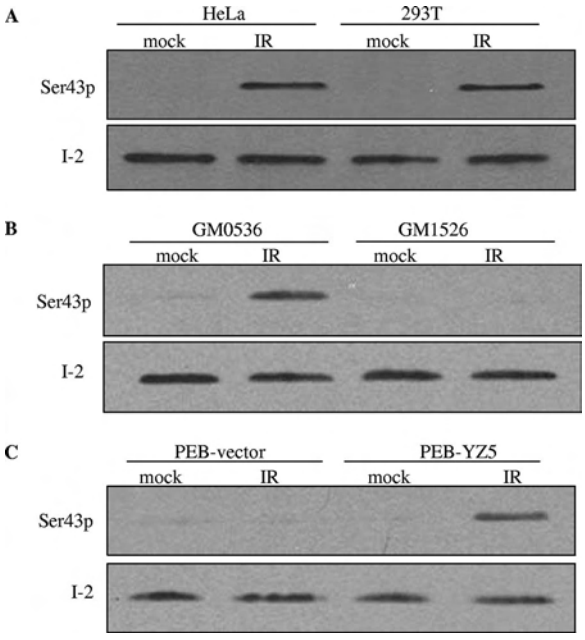


FIG. 3. ATM is required for IR-induced I-2 serine 43 phosphorylation. Shown are Western blot analyses of nuclear extracts from HeLa cells, 293T cells, EBV-transformed lymphoblast cell lines proficient (GM0536) and deficient (GM1526) in ATM, and SV40-transformed human fibroblast isogenic cell lines PEB-vector (ATM deficient) and PEB-YZ5 (expressing reconstituted ATM) with the phospho-serine 43 antibody (Ser43p).

phorylates I-2 at serine 43 in vitro and there is an ATM-dependent phosphorylation of this site in vivo after IR.

**ATM phosphorylation of I-2 at serine 43 is required for IR-induced PP1–I-2 dissociation and PP1 activation.** To assess the functional significance of the ATM phosphorylation of I-2, we explored the effects of ATM-dependent I-2 phosphorylation on the PP1–I-2 complex. 293T cells were transiently transfected with Xpress-tagged constructs expressing either a wild-type or a serine 43-to-alanine (S43A) mutant form of I-2, with or without IR. The exogenous I-2 was immunoprecipitated, and the immunoprecipitates were probed with the anti-Xpress or anti-PP1 antibodies. While wild-type I-2 brought down PP1 in the absence of IR, Xpress-tagged wild-type I-2 no longer bound to PP1 after DNA damage. In contrast, the S43A mutant form of I-2 remained bound to endogenous PP1 after IR (Fig. 4A). A reciprocal experiment showed that PP1 still associated with S43A mutant I-2 after IR (Fig. 4B). These observations demonstrate that ATM-mediated I-2 phosphorylation on serine 43 is required for the dissociation process of the PP1–I-2 complex in response to IR-induced DNA damage.

We then investigated whether serine 43 phosphorylation of I-2 was required for IR-induced PP1 activation. We transfected 293T cells with wild-type or S43A mutant I-2 and assessed potential dominant-inhibitory effects on PP1 activity. 293T cells transiently transfected with either vector only or vectors expressing wild-type I-2 exhibited normal IR-induced PP1 activation. In contrast, cells transfected with vectors expressing the S43A form of I-2 exhibited substantially impaired PP1 activation after IR (Fig. 4C). Thus, S43A mutant I-2 has dominant-inhibitory effects on endogenous PP1 activation after IR, demonstrating that ATM-mediated I-2 phosphorylation is required for IR-induced PP1 activation.

To further study in vivo activation of PP1 toward its substrates, we assessed the dephosphorylation of histone H1, a process mediated by PP1 (24). A flow cytometry-based assay was employed to measure H1 phosphorylation in the absence or presence of DNA damage. We found that H1 phosphorylation was significantly reduced after IR. Expressing vector only or wild-type I-2 did not alter the IR-induced inhibition of H1 phosphorylation, while expressing S43A mutant I-2 abolished the process (see Fig. S3 in the supplemental material). Therefore, our data demonstrate that in vivo PP1 activity is enhanced by ATM-mediated phosphorylation of I-2 after DNA damage.

**ATM phosphorylation of I-2 is critical for IR-induced PP1 threonine 320 dephosphorylation.** It was shown previously that nuclear PP1 contains the consensus sequence for phosphorylation by Cdk2 (9). PP1 threonine 320 phosphorylation inactivates PP1, and phosphorylation is attenuated after DNA damage in an ATM-dependent manner. Whether ATM-mediated I-2 phosphorylation interacts with the ATM-dependent inhibition of PP1 threonine 320 phosphorylation is not clear. To test this possibility, we performed experiments with 293T cells expressing vector only or wild-type or S43A mutant I-2 to investigate the change in threonine 320 phosphorylation after IR. We found that the S43A mutation can abolish IR-induced threonine 320 dephosphorylation (Fig. 5), suggesting that ATM-mediated I-2 serine 43 phosphorylation may function as an upstream cascade of the signaling pathway.

**ATM phosphorylation of I-2 at serine 43 is required for the IR-induced $G_2$/M checkpoint.** Previously, we reported that the ATM-dependent $G_2$/M checkpoint is correlated with the down-regulation of histone H3 serine 10 phosphorylation (30, 31). However, how ATM links to H3 serine 10 phosphorylation was not known. Since PP1 is considered to be the major phosphatase required for the down-regulation of serine 10 phosphorylation (10) and the activation of PP1 is associated with the down-regulation of H3 serine 10 phosphorylation (see Fig. S4 in the supplemental material), it seemed likely that ATM-mediated I-2 serine 43 phosphorylation after IR would be important for the inhibition of H3 serine 10 phosphorylation in response to IR. To test this hypothesis, we transfected HeLa cells with the wild-type or the S43A mutant form of I-2 and performed a flow cytometry analysis using an anti-phospho-H3 serine 10 antibody. We found that cells expressing vector only or wild-type I-2 showed robust down-regulation of H3 phosphorylation and activation of the $G_2$/M checkpoint after IR. However, cells expressing the dominant negative form of I-2 (the S43A mutant form) displayed no significant reduction in histone H3 phosphorylation in response to IR (Fig. 6A). These observations demonstrate a role for ATM-dependent I-2 serine 43 phosphorylation in the regulation of histone H3 serine 10 phosphorylation and the $G_2$/M checkpoint in response to DNA damage.

We also explored whether PP1 activation regulated the Aurora-B kinase, the kinase essential for H3 serine 10 phosphorylation. It was shown previously that Aurora-B was inhibited after IR-induced DNA damage (18). We found that IR-induced Aurora-B inhibition required functional ATM (Fig.

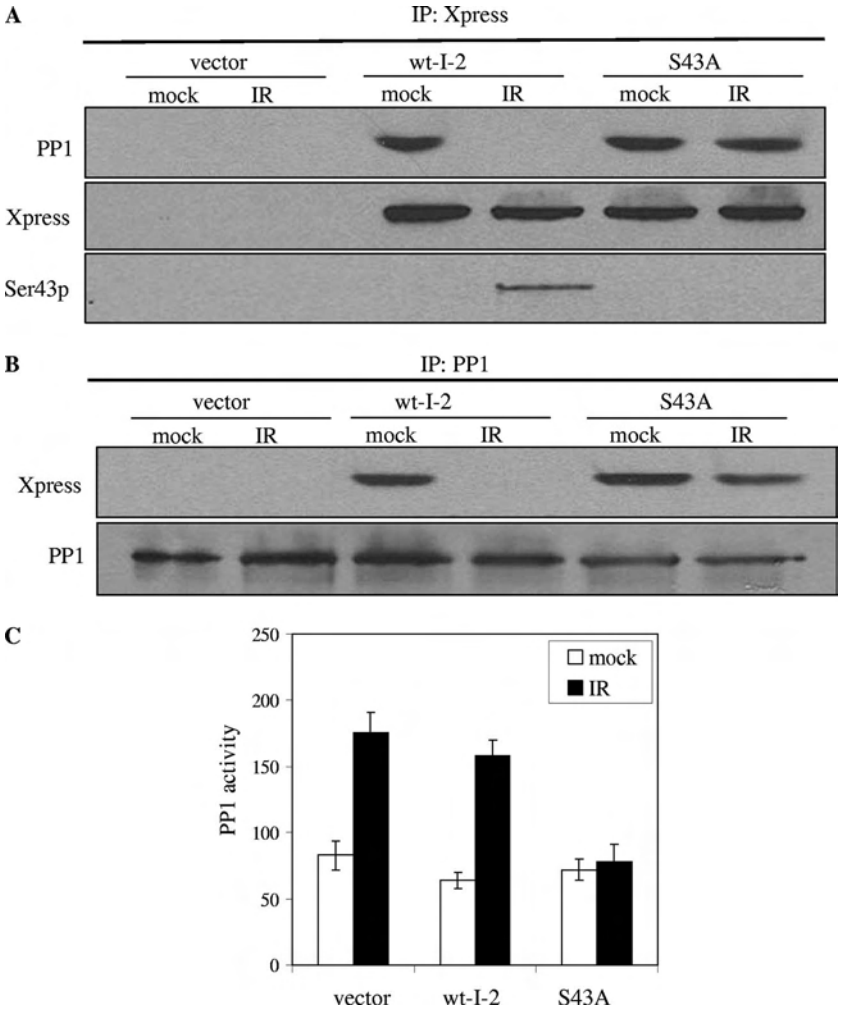


FIG. 4. ATM phosphorylation of I-2 at serine 43 is required for the dissociation of the PP1–I-2 complex and the activation of PP1. 293T cells were transfected with an empty vector or the Xpress-tagged wild-type or S43A mutant form of I-2 and mock treated (0 Gy) or treated with IR (6 Gy). (A) The exogenous I-2 was immunoprecipitated with an anti-Xpress antibody, and the immunoprecipitates (IP) were probed with an anti-PP1 or anti-Xpress antibody. wt-I-2, wild-type I-2; Ser43p, phospho-serine 43 antibody. (B) Endogenous PP1 was immunoprecipitated with anti-PP1, and the immunoprecipitates were probed with anti-PP1 or anti-Xpress antibodies. (C) Endogenous PP1 was immunoprecipitated and subjected to in vitro phosphatase assays. Error bars represent ±1 standard deviation, and the means of results from three independent experiments are graphed.

6B). Further, cells expressing the S43A mutant form of I-2 did not show the inhibition of Aurora-B compared to that in the appropriate controls (Fig. 6C). These observations demonstrate that ATM-mediated I-2 phosphorylation and PP1 activity can inhibit Aurora-B kinase activity, thereby causing reduced H3 phosphorylation and activation of the $G_2$/M checkpoint.

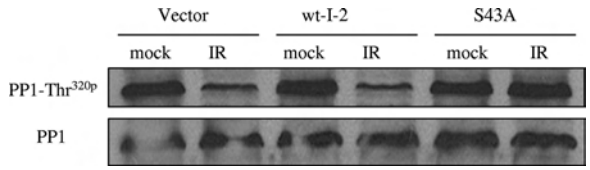


FIG. 5. ATM phosphorylation of I-2 at serine 43 is required for the dephosphorylation of PP1 threonine 320 in response to DNA damage. 293T cells were transiently transfected with an empty vector, Xpress-tagged wild-type I-2 (wt-I-2), or S43A mutant I-2 and treated without or with IR (6 Gy). Nuclear extracts were subjected to immunoblotting using anti-phospho-threonine 320 (PP1-Thr$^{320p}$) or anti-PP1 antibody.

## DISCUSSION

Dissecting ATM-mediated signaling pathways in the cellular response to DNA damage can provide important insights into how the loss of ATM function causes such a devastating disease, ataxia-telangiectasia (A-T), in humans. Upon DNA damage, ATM binds strongly to damaged sites and its kinase activity is enhanced. Activated ATM in turn phosphorylates a list of substrates in pathways that together ensure cellular survival and recovery. A number of ATM-mediated signaling pathways have been revealed, and the functional significance of these pathways has been studied extensively. However, due to the complexity of the A-T phenotypes, detailed mechanisms on

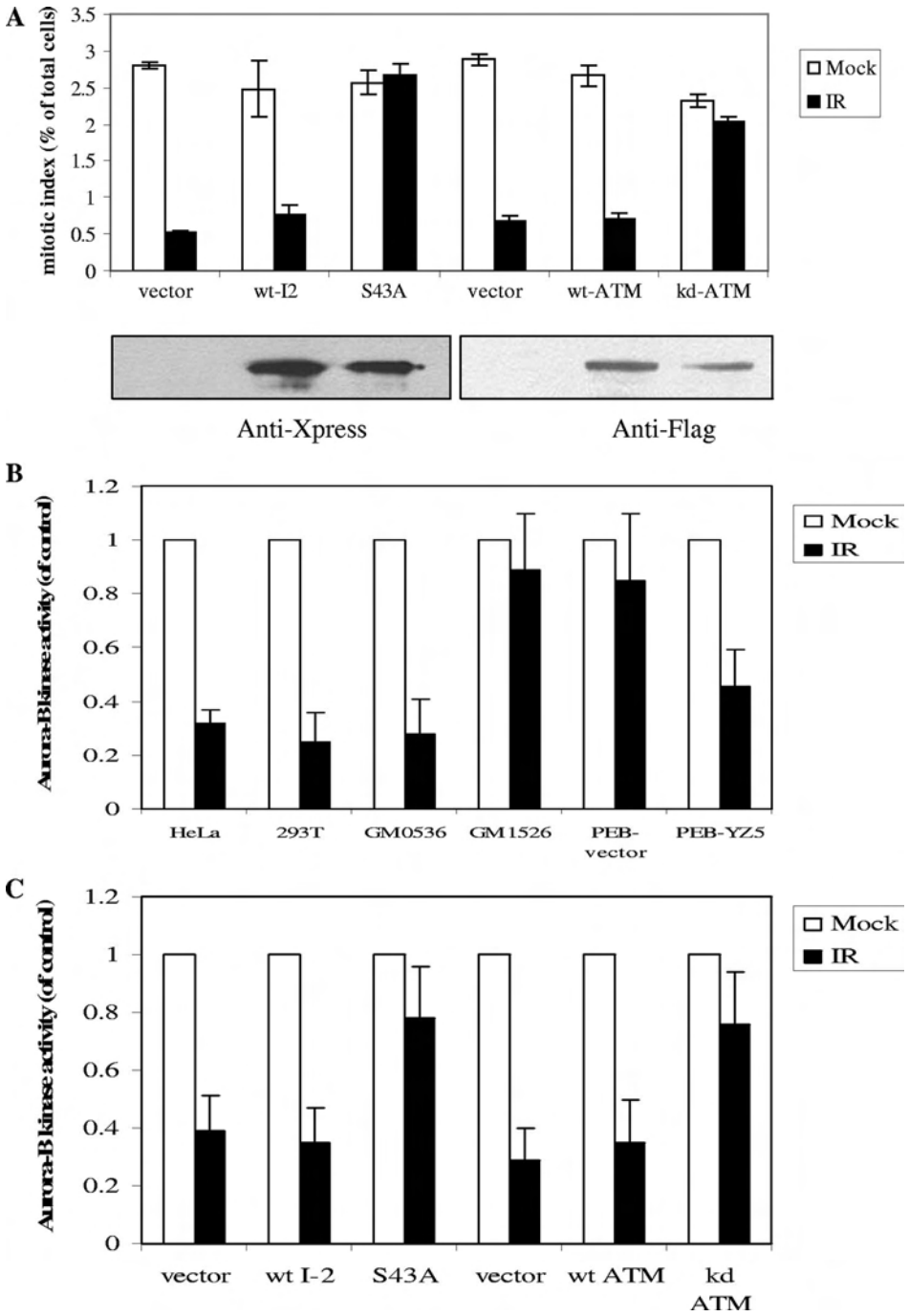


FIG. 6. ATM phosphorylation of I-2 is required for the activation of the $G_2$/M checkpoint and the inhibition of Aurora-B in response to IR-induced DNA damage. (A) HeLa cells were transfected with an empty vector, Xpress-tagged wild-type I-2 (wt-I2), the S43A mutant form of I-2 (S43A), wild-type ATM (wt-ATM), or kinase-dead ATM (kd-ATM) and treated without IR or with IR (6 Gy). Ninety minutes after IR, cells were harvested and subjected to the flow cytometry-based phospho-histone H3 staining assay. Error bars represent ±1 standard deviation, and the means of results from three independent experiments are graphed. Shown under the bar graph are the Western blot results demonstrating the expression patterns of the exogenous proteins. (B) Cells were treated without or with IR (6 Gy), and Aurora-B was immunoprecipitated and subjected to in vitro kinase assays using histone H3 as the substrate. Phosphorylation signals were quantified by a phosphorimager. (C) HeLa cells were transfected with an empty vector, the Xpress-tagged wild-type or S43A mutant form of I-2, or wild-type or kinase-dead ATM and treated without IR or with IR (6 Gy). The Aurora-B kinase assays were performed 90 min after IR. In panels B and C, values for activity levels are shown relative to the activity level of the control, which was set at 1.

how the loss of ATM leads to a variety of A-T phenotypes remains to be further explored. In this report, we highlight a novel signaling pathway that involves ATM, PP1, and I-2. We demonstrate that I-2 is a substrate of ATM and that ATM phosphorylation of I-2 at serine 43 is required for the activation of PP1 in response to DNA damage.

Previously, we reported a rapid and ATM-dependent $G_2$/M checkpoint that correlates with the down-regulation of histone

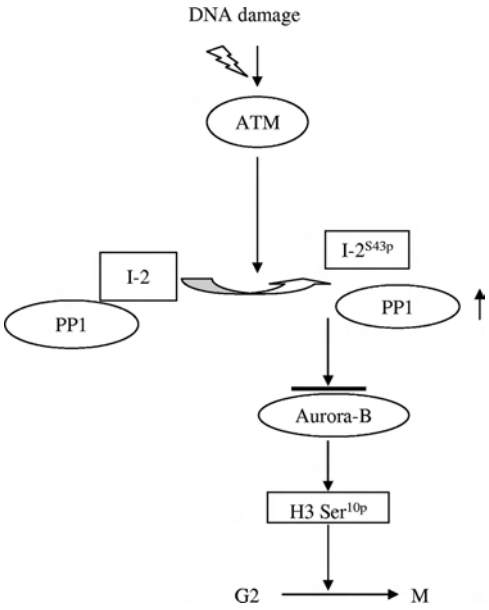


FIG. 7. Proposed role of ATM-mediated I-2 phosphorylation in the activation of PP1 and the signaling cascade in $G_2$/M checkpoint regulation in response to IR-induced DNA damage. I-$2^{S43p}$, I-2 phosphorylated at serine 43; H3 $Ser^{10p}$, H3 serine 10 phosphorylation.

H3 serine 10 phosphorylation in response to IR (30). However, how ATM links to regulators of histone H3 serine 10 phosphorylation was not known. It was reported previously that the enzymatic activities of PP1 are activated in response to IR in an ATM-dependent manner (9) and that Cdk2-mediated PP1 threonine 320 phosphorylation is attenuated after DNA damage. However, a detailed mechanism of ATM-mediated PP1 activation in response to DNA damage remained unknown. Starting with investigations of IR-induced PP1 activity, we found that IR induced an ATM-dependent dissociation of the PP1–I-2 complex. Further studies showed that ATM phosphorylated I-2 on serine 43 and that this phosphorylation led to the dissociation of the complex and the activation of PP1. This effect, in turn, resulted in the inhibition of Aurora-B, the down-regulation of histone H3 serine 10 phosphorylation, and the activation of the $G_2$/M checkpoint (Fig. 7).

Our data also demonstrate that ATM-mediated I-2 phosphorylation is an essential step for the attenuation of IR-induced threonine 320 phosphorylation. One possible explanation is that, after the dissociation of the PP1–I-2 complex, PP1 initiates autodephosphorylation which eventually activates the phosphatase. More-detailed investigations are required to determine whether threonine 320 dephosphorylation may also play a role in ATM-mediated I-2 phosphorylation and PP1–I-2 dissociation.

PP1 activity is also controlled by other regulatory subunits, such as I-1, NIPP1, and DARPP32 (21). Whether these regulators are involved in the DNA damage response and whether they dissociate from PP1 are not known. It is reasonable to suspect that some inhibitors are also involved in regulating PP1 activity in response to DNA damage. For example, I-1 has been shown previously to regulate cell growth and has been linked to PP1 in the $G_1$ cell cycle control (21).

Histone H3 serine 10 phosphorylation is critical for chromosome condensation and segregation, and it has been used previously as a mitotic marker for studying the activation of the $G_2$/M checkpoint. Our data demonstrate that the activation of PP1 governed by ATM phosphorylation of I-2 leads to the down-regulation of H3 serine 10 phosphorylation. We also found that activated PP1 leads to the inhibition of the Aurora-B kinase. Therefore, PP1 may prevent H3 phosphorylation to delay the transition from $G_2$ to M, thereby activating the $G_2$/M checkpoint. However, it is also possible that activated PP1 may directly dephosphorylate the phosphorylated H3 when cells are already in the M phase. Therefore, PP1 and I-2 serine 43 phosphorylation may also have a role to facilitate the mitotic exit. The latter scenario is supported by the evidence that yeast PP1 homolog Dis2 can down-regulate Chk1 activity for a checkpoint release (6). Therefore, the detailed mechanisms of ATM-mediated PP1 activation in the regulation of histone H3 serine 10 phosphorylation remain to be further investigated.

The functional significance of ATM-mediated phosphorylation of I-2 and activation of PP1 activity may extend beyond the roles of these processes in histone H3 modification and cell cycle checkpoint regulation. Since PP1 is a major eukaryotic protein serine/threonine phosphatase that regulates a variety of cellular functions, the regulation of PP1 through ATM phosphorylation of I-2 may have a significant impact on many cellular responses to DNA damage. Dephosphorylation by phosphatases can turn signals off or regulate the degradation of phosphorylated substrates, thus balancing the physiological effects of kinases (19).

One of the known physiological roles of I-2 is to control sperm motility (28). A testis-specific isoform of PP1 forms an inactive complex with I-2, and GSK-3-mediated I-2 phosphorylation which activates the PP1–I-2 complex results in an increase in the PP1 activity seen in nonmotile immature sperm. The exposure of the immature sperm to phosphatase inhibitors, such as okadaic acid and calyculin A, induces motility, suggesting that I-2 inhibits PP1 activity in mature mammalian sperm cells to facilitate their motility. The PP1–I-2 complex is also involved in insulin signaling (5, 20). These observations are particularly interesting since both A-T patients and A-T mice are sterile and have glucose intolerance and insulin resistance (26), suggesting a physiologically important link between ATM and PP1–I-2. Indeed, we have observed that ATM phosphorylates I-2 at serine 43 in response to insulin stimulation (unpublished data). The establishment of a serine 43 phosphorylation mutant knock-in mouse model to study the physiological significance of ATM-mediated I-2 phosphorylation is under way.

In summary, our data provide mechanistic insights into the activation process of PP1 in DNA damage response pathways in mammalian cells. The results of these studies also provide a foundation for future studies of the ATM–PP1–I-2 pathway in regulating cellular responses to stress.

## ACKNOWLEDGMENTS

We thank Yosef Shiloh for providing the isogenic fibroblast cell lines deficient or proficient in ATM. We also thank Ratna K. Vadlamudi for providing reagents for constructing the Xpress-tagged I-2. We thank Jaideep Thottassery for helpful discussions.

This work was supported in part by grants from the National Institutes of Health (RR020152-01, CA71387, CA21765, and ES013301) and by the Department of Defense grant W81XWH-05-1-0018.

## REFERENCES


1. **Alessi, D. R., A. J. Street, P. Cohen, and P. T. Cohen.** 1993. Inhibitor-2 functions like a chaperone to fold three expressed isoforms of mammalian protein phosphatase-1 into a conformation with the specificity and regulatory properties of the native enzyme. Eur. J. Biochem. **213:**1055–1066.
2. **Ali, A., J. Zhang, S. Bao, I. Liu, D. Otterness, N. M. Dean, R. T. Abraham, and X. F. Wang.** 2004. Requirement of protein phosphatase 5 in DNA-damage-induced ATM activation. Genes Dev. **18:**249–254.
3. **Cohen, P. T.** 2002. Protein phosphatase 1—targeted in many directions. J. Cell Sci. **115:**241–256.
4. **Cohen, P. T., N. D. Brewis, V. Hughes, and D. J. Mann.** 1990. Protein serine/threonine phosphatases; an expanding family. FEBS Lett. **268:**355–359.
5. **Delibegovic, M., C. G. Armstrong, L. Dobbie, P. W. Watt, A. J. Smith, and P. T. Cohen.** 2003. Disruption of the striated muscle glycogen targeting subunit PPP1R3A of protein phosphatase 1 leads to increased weight gain, fat deposition, and development of insulin resistance. Diabetes **52:**596–604.
6. **Den Elzen, N. R., and M. J. O'Connell.** 2004. Recovery from DNA damage checkpoint arrest by PP1-mediated inhibition of Chk1. EMBO J. **23:**908–918.
7. **Falck, J., N. Mailand, R. G. Syljuasen, J. Bartek, and J. Likas.** 2001. The ATM-Chk2-Cdc25A checkpoint pathway guards against radioresistant DNA synthesis. Nature **410:**842–847.
8. **Goodarzi, A. A., J. C. Jonnalagadda, P. Douglas, D. Young, R. Ye, G. B. Moorhead, S. P. Lees-Miller, and K. K. Khanna.** 2004. Autophosphorylation of ataxia-telangiectasia mutated is regulated by protein phosphatase 2A. EMBO J. **23:**4451–4461.
9. **Guo, C. Y., D. L. Brautigan, and J. M. Larner.** 2002. Ionizing radiation activates nuclear protein phosphatase-1 by ATM-dependent dephosphorylation. J. Biol. Chem. **277:**41756–41761.
10. **Hsu, J. Y., Z. W. Sun, X. Li, M. Reuben, K. Tatchell, D. K. Bishop, J. M. Grushcow, C. J. Brame, J. A. Caldwell, D. F. Hunt, R. Lin, M. M. Smith, and C. D. Allis.** 2000. Mitotic phosphorylation of histone H3 is governed by Ipl1/aurora kinase and Glc7/PP1 phosphatase in budding yeast and nematodes. Cell **102:**279–291.
11. **Huang, F. L., and W. H. Glinsmann.** 1976. Separation and characterization of two phosphorylase phosphatase inhibitors from rabbit skeletal muscle. Eur. J. Biochem. **70:**419–426.
12. **Kim, S.-T., D.-S. Lim, C. E. Canman, and M. B. Kastan.** 1999. Substrate specificities and identification of putative substrates of ATM kinase family members. J. Biol. Chem. **274:**37538–37543.
13. **Kim, S. T., B. Xu, and M. B. Kastan.** 2002. Involvement of the cohesin protein, Smc1, in Atm-dependent and independent responses to DNA damage. Genes Dev. **16:**560–570.
14. **Kurz, E. U., and S. P. Lees-Miller.** 2004. DNA damage-induced activation of ATM and ATM-dependent signaling pathways. DNA Repair (Amsterdam) **3:**889–900.
15. **Leach, C., S. Shenolikar, and D. L. Brautigan.** 2003. Phosphorylation of phosphatase inhibitor-2 at centrosomes during mitosis. J. Biol. Chem. **278:**26015–26020.
16. **MacKintosh, C., A. J. Garton, A. McDonnell, D. Barford, P. T. Cohen, N. K. Tonks, and P. Cohen.** 1996. Further evidence that inhibitor-2 acts like a chaperone to fold PP1 into its native conformation. FEBS Lett. **397:**235–238.
17. **Matsuoka, S., B. A. Ballif, A. Smogorzewska, E. R. McDonald III, K. E. Hurov, J. Luo, C. E. Bakalarski, Z. Zhao, N. Solimini, Y. Lerenthal, Y. Shiloh, S. P. Gygi, and S. J. Elledge.** 2007. ATM and ATR substrate analysis reveals extensive protein networks responsive to DNA damage. Science **316:**1160–1166.
18. **Monaco, L., U. Kolthur-Seetharam, R. Loury, J. M. Murcia, M. G. de, and P. Sassone-Corsi.** 2005. Inhibition of Aurora-B kinase activity by poly(ADP-ribosyl)ation in response to DNA damage. Proc. Natl. Acad. Sci. USA **102:**14244–14248.
19. **Moorhead, G. B., L. Trinkle-Mulcahy, and A. Ulke-Lemee.** 2007. Emerging roles of nuclear protein phosphatases. Nat. Rev. Mol. Cell Biol. **8:**234–244.
20. **Munro, S., D. J. Cuthbertson, J. Cunningham, M. Sales, and P. T. Cohen.** 2002. Human skeletal muscle expresses a glycogen-targeting subunit of PP1 that is identical to the insulin-sensitive glycogen-targeting subunit G(L) of liver. Diabetes **51:**591–598.
21. **Oliver, C. J., and S. Shenolikar.** 1998. Physiologic importance of protein phosphatase inhibitors. Front. Biosci. **3:**D961–D972.
22. **O'Neill, T., A. J. Dwyer, Y. Ziv, D. W. Chan, S. P. Lees-Miller, R. H. Abraham, J. H. Lai, D. Hill, Y. Shiloh, L. C. Cantley, and G. A. Rathbun.** 2000. Utilization of oriented peptide libraries to identify substrate motifs selected by ATM. J. Biol. Chem. **275:**22719–22727.
23. **Park, I. K., and A. A. Paoli-Roach.** 1994. Domains of phosphatase inhibitor-2 involved in the control of the ATP-Mg-dependent protein phosphatase. J. Biol. Chem. **269:**28919–28928.
24. **Paulson, J. R., J. S. Patzlaff, and A. J. Vallis.** 1996. Evidence that the endogenous histone H1 phosphatase in HeLa mitotic chromosomes is protein phosphatase 1, not protein phosphatase 2A. J. Cell Sci. **109:**1437–1447.
25. **Shiloh, Y., and M. B. Kastan.** 2001. ATM: genome stability, neuronal development, and cancer cross paths. Adv. Cancer Res. **83:**209–254.
26. **Shiloh, Y.** 2006. The ATM-mediated DNA-damage response: taking shape. Trends Biochem. Sci. **31:**402–410.
27. **Taniguchi, T., I. Garcia-Higuera, B. Xu, P. R. Andreassen, R. C. Gregory, S. T. Kim, W. S. Lane, M. B. Kastan, and A. D. D'Andrea.** 2002. Convergence of the fanconi anemia and ataxia telangiectasia signaling pathways. Cell **109:**459–472.
28. **Vijayaraghavan, S., D. T. Stephens, K. Trautman, G. D. Smith, B. Khatra, E. F. da Cruz e Silva, and P. Greengard.** 1996. Sperm motility development in the epididymis is associated with decreased glycogen synthase kinase-3 and protein phosphatase 1 activity. Biol. Reprod. **54:**709–718.
29. **Wang, H., and D. L. Brautigan.** 2002. A novel transmembrane Ser/Thr kinase complexes with protein phosphatase-1 and inhibitor-2. J. Biol. Chem. **277:**49605–49612.
30. **Xu, B., S.-T. Kim, and M. B. Kastan.** 2001. Involvement of Brca1 in S-phase and $G_2$-phase checkpoints after ionizing irradiation. Mol. Cell. Biol. **21:**3445–3450.
31. **Xu, B., S. T. Kim, D. S. Lim, and M. B. Kastan.** 2002. Two molecularly distinct G(2)/M checkpoints are induced by ionizing irradiation. Mol. Cell. Biol. **22:**1049–1059.
32. **Xu, B., A. H. O'Donnell, S. T. Kim, and M. B. Kastan.** 2002. Phosphorylation of serine 1387 in Brca1 is specifically required for the Atm-mediated S-phase checkpoint after ionizing irradiation. Cancer Res. **62:**4588–4591.
33. **Yazdi, P. T., Y. Wang, S. Zhao, N. Patel, E. Y. Lee, and J. Qin.** 2002. SMC1 is a downstream effector in the ATM/NBS1 branch of the human S-phase checkpoint. Genes Dev. **16:**571–582.
34. **Zhang, J., S. Bao, R. Furumai, K. S. Kucera, A. Ali, N. M. Dean, and X. F. Wang.** 2005. Protein phosphatase 5 is required for ATR-mediated checkpoint activation. Mol. Cell. Biol. **25:**9910–9919.